The development of a space climatology: 3. Models of the evolution of distributions of space weather variables with timescale

Space Weather

Supporting Information for

The development of a space climatology: 3. Models of the evolution of distributions of space weather parameters with timescale

Mike Lockwood[1], Sarah N. Bentley[1], Mathew J. Owens[1], Luke A. Barnard[1], Chris J. Scott[1], Clare E. Watt[1], Oliver Allanson[1] and Mervyn P. Freeman[2]

Paper accepted by Space Weather, September 2018.

[1]Department of Meteorology, University of Reading, Earley Gate, P.O. Box 243, Reading, Berkshire, RG6 6BB, UK

[2] British Antarctic Survey, High Cross, Madingley Road, Cambridge, CB3 0ET, UK.

Contents of this file

1. Maximum Likelihood Estimation (MLE) fitting

2. Results of fitting 7 standard distributions to the data

3. A Table listing the largest geomagnetic storms in rank order defined by daily mean *ap* values, *Ap*.

Introduction

Part 1

This supporting information gives details of the Maximum Likelihood Estimation (MLE) method and associated goodness-of-fit metrics

Part 2

The values of best-fit parameters (and their uncertainties) and the goodness-of-fit metrics are presented for the fits of 7 selected distribution forms to the observed distributions of the geomagnetic indices, *ap* and *Dst* and the estimated power into the magnetosphere, P_α (all expressed as ratios of their annual means). The procedures are repeated for data averaged over timescales τ of 3 hours, 1 day, 7 days, 27 days, 0.5 years and 1 year. Plots of the observed and fitted distributions (both probability density functions (p.d.f.s) and cumulative distribution functions (c.d.f.s) are also presented for all cases.

Part 3

A Table giving a list in rank order of the 83 largest storms (the top 0.25%) defined by daily mean ap values, *Ap*

Part 1. Maximum Likelihood (MLE) method and associated goodness-of-fit metrics

Probability density distributions can be fitted to data using the least squares method. This involves counting the fraction of all samples in bins, P_o, of arbitrarily-chosen width to create a histogram and then evaluating the adopted pdf function for the bin centers, P_m. The mean square of the deviation is then computed, $\Delta = \langle (P_m - P_o)^2 \rangle$ and the parameters describing the fitted distribution iterated until the minimum Δ, Δ_{MS}, is obtained. One major problem with this "last squares" fit is that the results can depend on the bin width chosen [e.g., *Woody et al.*, 2016] and it assumes that the fit residuals are normally distributed.

Maximum Likelihood Estimation (MLE) provides an alternative that avoids these problems. It is a generalization of the least squares method, which it reduces to if all the assumptions of least squares are met. MLE searches for the parameter values of the distribution form used that maximize a likelihood function, given the observations. The likelihood is estimated from the joint probability of the assumed distribution generating the N observed data points x_1, x_2, ...x_i, ...x_N for a parameter a. (For simplicity we here consider a distribution with just one fit parameter, a: in general there can be several). For independent measurements this is given by the product of the individual densities $p(x|a)$, which is the likelihood

$$L(a) = p(x_1|a) \times p(x_2|a) \; \ldots\ldots \times p(x_i|a) \; \ldots\ldots \times p(x_N|a) = \prod_{i=1}^{N} p(x_i|a)$$

For a number of reasons is easier to work with natural logarithm of L, the log-likelihood $F(a)$

$$F(a) = \log_n(L) = \Sigma_{i=1}^{N} \log_n(p(x_i|a))$$

MLE finds the parameter value a that maximizes $L(a)$, the maximum likelihood being L_m

There are two goodness-of-fit metrics that can be used in MLE. The *AIC* is the Akaike Information Criterion metric and the *BIC* the Bayesian (or Schwarz) Information Criterion. Where

$$AIC = 2d_f - 2\log_n(L_m)$$

where d_f is the number of fit parameters (degrees of freedom) and

$BIC = \log_n(N)\times d_f - 2\log_n(L_m)$

The AIC and BIC values are not (unlike Δ_{MS}) absolute quality metrics because they depend on the data sample set of x values in question. However, they can be used to compare the goodness-of-fit of different distributions to the same set of x data, the smallest value indicating the largest maximum likelihood L_m. The first term means that the number of degrees of freedom of the fit are allowed for and the BIC in gives larger weight to this factor than the AIC provided the number of samples N exceeds 7. Hence AIC and BIC are useful in evaluation which distribution best fits the data.

One other goodness-of-fit test we apply is the modified Kolmogorov–Smirnov test which yields the metric D which is the largest absolute value of the difference of the observed and fitted cumulative distribution functions (c.d.f.s). These c.d.f.s can be evaluated without binning the data and the K-S test is a non-parametric test as it does not assume that the data are normally distributed.

Part 2. Results of maximum likelihood (MLE) fitting to observed distributions of geomagnetic indices *ap* and *Dst* and of the power input into the magnetosphere, P_α

This section presents Tables giving best-fit parameters and their 2-σ uncertainty ranges and the goodness of fit metrics (and their rank orders) for 7 different standard distribution forms. The forms used are:

normal (Gaussian) distribution
lognormal distribution
Weibull distribution
Burr distribution
Gamma distribution
Log-logistic distribution
Rician distribution

For all these distributions the number of degrees of freedom is $d_f = 2$, except the Burr for which $d_f = 3$. These distributions are fitted to the ratios of observed $<ap>_\tau/<ap>_{\tau=1yr}$, $<Dst>_\tau/<Dst>_{\tau=1yr}$, and $<P_\alpha>_\tau/<P_\alpha>_{\tau=1yr}$ - in each case for 6 different values of averaging timescale τ, namely: 3hrs (the basic resolution of the *ap* data), 1 day, 7 days, 27 days, 0.5 year and 1 year. In each case, a plot is given of both the observed and best-fit (MLE) cumulative distribution functions (c.d.f.s) and of the corresponding probability density functions (p.d.f.s). Note that in the case of the observed p.d.f.s, the data samples have been binned (to give a histogram) into 150 contiguous bins centered on [0.5:1:150](x_{98}/100) where x_{98} is the 98th percentile of the observed distribution and the numbers of samples n in each bin then normalized so that $\Sigma n(x_{98}/100)$ is unity.

For the distributions of $<ap>_\tau/<ap>_{\tau=1yr}$, the lognormal distribution form consistently performs best in all four metrics until τ gets large and the distribution becomes close to normal. Note that in these large-τ cases, the AIC and BIC have both turned negative because the maximum likelihood, L_m exceeds unity. (It is often said that L_m cannot exceed unity but this is incorrect and this means that the log likelihood can be positive). However, this only happens when the fits are of extremely high quality (as seen in the plots). As all the tested distributions tend to Gaussians in one limit, all distributions fit the high τ distributions very well and the rank orders are based on minimal differences in the metrics – i.e. the fitted distributions are essentially all equally valid. Note for τ = 1 year the distribution of and parameter $<x>_{\tau}/<x>_{\tau=1yr}$, is a delta function at unity which is a Gaussian of unity mean 1 and standard deviation zero.

The behavior is quite similar for the distributions of normalized power input to the magnetosphere $<P_{\alpha}>_{\tau}/<P_{\alpha}>_{\tau=1yr}$, except at the lowest τ where the lognormal does not fit the observations well. For τ of 7 days and 27 days the lognormal is best by all metrics and, as for *ap*, at the larger τ all distributions fit the near-Gaussian form well and the lognormal is, effectively, as good as any other form. The distribution at τ = 3 hours is complex in form and in Paper 2 is explained as the effect of averaging (via the central limit theorem) on the very non-standard distribution at τ = 1 min in the IMF orientation factor. In Paper 2 it was described in terms of a Weibull distribution which fits the above-the-mode values very well but does not fit the mode and below quite as well as the Burr distribution (see Figures S13 and S14). Table S6 shows that both the *AIC* and *BIC* metrics indicate that the addition of an extra shape parameter in the Burr is valid in this case. The advantage gained in using the Burr is a better fitting of the near-zero peak but the fits to the distribution above the mode are very similar.

In contrast, for the distributions of $<Dst>_{\tau}/<Dst>_{\tau=1yr}$, the lognormal distribution is never the best option. Of the two-parameter distribution fits the Gamma and the Weibull distributions are very similar in all their goodness of fit estimates and the best options for τ up to 0.5 year, above which all distributions fit the near-Gaussian observed distribution well. However, at 7 days and below the Burr distribution is best, even in the *BIC* metric that penalises the extra degree of freedom most. The Figures S7 to S11 show that the 2-parameter fits match the distribution above the mode well but have trouble matching the exact form of the peak around the mode.

Table S1. Best-fit parameters and their 2-σ uncertainty ranges for 7 tested distribution forms fitted to the ratio $<ap>_{\tau}/<ap>_{\tau=1yr}$ for the *ap* geomagnetic index data for 6 different values of τ. The distributions studied are: the normal (Gaussian) distribution (for which the parameter *A* is the mean, *m*; and parameter *B* is the standard deviation, σ); the Lognormal distribution ($A = \mu$, the mean of logarithmic values; $B = \sigma$, the standard deviation of logarithmic values); the Weibull ($A = \lambda$, the scale parameter; and $B = k$, the shape parameter); the Burr distribution ($A = \lambda$, the scale parameter, $B = k_1$, the first shape parameter, and $C = k_2$, a second shape parameter); the Gamma distribution ($A = k$, the shape parameter, and $B = \lambda$, the scale parameter); the Log-logistic distribution ($A = m$, the mean; and $B = k$, the shape parameter); and the Rician distribution ($A = s$, the noncentrality parameter and $B = \lambda$, the scale parameter). In each case the optimum fit is given, along with the minimum and maximum of the 2-σ uncertainty range, as derived using the Maximum Likelihood Estimation (MLE) method (using the MATLAB statistics toolbox). Fits are carried out using averaging intervals of τ of 3hrs (the basic resolution of the *ap* data), 1 day, 7 days, 27 days, half a year and 1 year.

1	2	3	4	5	6	7	8	9	10	11	12
distribution		**time**	**best**	**Min**	**max**	**Best**	**min**	**max**	**best**	**min**	**Max**
		τ	***A***	***A***	***A***	***B***	***B***	***B***	***C***	***C***	***C***
Normal	ap	3 hrs	1.0353	1.0298	1.0407	1.3642	1.3604	1.3681			
Lognormal	ap	3 hrs	-0.4054	-0.4089	-0.4018	0.8845	0.882	0.887			
Weibull	ap	3 hrs	1.0546	1.0503	1.059	1.0382	1.0354	1.0411			
Burr	ap	3 hrs	0.4136	0.4093	0.4178	2.6086	2.5857	2.6318	0.5337	0.5252	0.5424
Gamma	ap	3 hrs	1.2773	1.2708	1.2838	0.8105	0.8055	0.8156			
LogLogistic	ap	3 hrs	-0.4452	-0.4488	-0.4416	0.5081	0.5064	0.5097			
Rician	ap	3 hrs	0.0232	0	0.0784	1.2109	1.2084	1.2134			
Normal	ap	1 dy	1.0006	0.9892	1.0119	1.0191	1.0112	1.0273			
Lognormal	ap	1 dy	-0.3305	-0.3393	-0.3216	0.7966	0.7903	0.8029			
Weibull	ap	1 dy	1.0758	1.0653	1.0864	1.2081	1.1988	1.2175			
Burr	ap	1 dy	0.6294	0.6103	0.6491	2.3578	2.311	2.4054	0.8394	0.8024	0.8782
Gamma	ap	1 dy	1.6576	1.6338	1.6818	0.6036	0.5935	0.6139			
LogLogistic	ap	1 dy	-0.3446	-0.3535	-0.3358	0.4532	0.449	0.4574			
Rician	ap	1 dy	0.0259	0	0.1757	1.0098	1.0038	1.0157			
Normal	ap	7 dy	1	0.9832	1.0168	0.5677	0.5561	0.5798			
Lognormal	ap	7 dy	-0.1312	-0.146	-0.1163	0.5034	0.4932	0.5142			
Weibull	ap	7 dy	1.1331	1.1145	1.1519	1.8972	1.8588	1.9364			
Burr	ap	7 dy	0.8082	0.7659	0.8529	3.6816	3.4895	3.8841	0.8465	0.7488	0.957
Gamma	ap	7 dy	3.9706	3.8145	4.133	0.2519	0.2413	0.2629			
LogLogistic	ap	7 dy	-0.1406	-0.1556	-0.1257	0.2891	0.2822	0.2962			
Rician	ap	7 dy	0.0285	0	0.7017	0.8129	0.7963	0.8299			
Normal	ap	27 dy	1	0.9819	1.0181	0.3113	0.2991	0.3247			
Lognormal	ap	27 dy	-0.0459	-0.0634	-0.0283	0.3023	0.2905	0.3154			
Weibull	ap	27 dy	1.1117	1.0911	1.1327	3.2846	3.1528	3.4218			
Burr	ap	27 dy	0.9507	0.8892	1.0165	5.8123	5.2627	6.4194	0.9908	0.7755	1.2658
Gamma	ap	27 dy	11.0589	10.2011	11.9889	0.0904	0.0833	0.0982			
LogLogistic	ap	27 dy	-0.0481	-0.0656	-0.0306	0.1726	0.1645	0.1811			
Rician	ap	27 dy	0.943	0.9229	0.9631	0.3222	0.3082	0.3369			
Normal	ap	0.5 yr	1	0.9811	1.0189	0.1242	0.1126	0.1395			
Lognormal	ap	0.5 yr	-0.0078	-0.0269	0.0113	0.1256	0.1138	0.141			
Weibull	ap	0.5 yr	1.0552	1.0362	1.0746	8.7762	7.8306	9.836			
Burr	ap	0.5 yr	1.1125	0.9492	1.3038	10.9177	8.515	13.9984	2.4749	0.7423	8.2519
Gamma	ap	0.5 yr	64.1512	51.8616	79.3531	0.0156	0.0126	0.0193			
LogLogistic	ap	0.5 yr	-0.0051	-0.0246	0.0144	0.0734	0.0649	0.0831			
Rician	ap	0.5 yr	0.9921	0.9732	1.0111	0.1247	0.112	0.1389			
Normal	ap	1 yr	1	0.9967	1.0033	0.0152	0.0133	0.0181			
Lognormal	ap	1 yr	-0.0001	-0.0035	0.0032	0.0154	0.0134	0.0182			
Weibull	ap	1 yr	1.0071	1.0036	1.0106	64.888	56.373	74.6887			
Burr	ap	1 yr	1.002	0.9947	1.0093	1307	99.1262	0.0002	1.1515	0.6154	2.1547
Gamma	ap	1 yr	4254.4	3144.1	5756.7	0.0002	0.0002	0.0003			
LogLogistic	ap	1 yr	0.0005	-0.0021	0.0031	0.0073	0.0061	0.0088			
Rician	ap	1 yr	0.9999	0.9966	1.0031	0.0152	0.0131	0.0177			

Table S2. Goodness-of-fit metrics for the 7 tested distribution forms and the *ap* geomagnetic index ratio $<ap>_\tau/<ap>_{\tau=1yr}$ data averaged over intervals of duration τ described in Table S1. *D* is the largest absolute value of the difference of the observed and fitted cumulative distribution functions (c.d.f.s) obtained from a modified version of the non-parametric Kolmogorov–Smirnov test; Δ_{MS} is the mean square deviation of the observed and fitted probability distribution functions (p.d.f.s) for 150 contiguous bins centered on $<ap>_\tau/<ap>_{\tau=1yr}$ = [0.5:1:150](x_{98}/100) where x_{98} is the 98th percentile of the observed $<ap>_\tau/<ap>_{\tau=1yr}$ distribution. *N* is the total number of available samples, *AIC* is the Akaike Information Criterion metric from the maximum likelihood estimate, and *BIC* the Bayesian Information Criterion. The last 4 columns give the rank order in goodness-of-fit for a given τ according to these four metrics. Note all distributions have two degrees of freedom, except the Burr that has 3.

1	2	3	4	5	6	7	8	9	10	11	12
distribution		**Time**	**Goodness of fit tests**					**Rank**			
		τ	*D*	D_{MS}	*N*	*AIC*	*BIC*	*D*	Δ_{MS}	*AIC*	*BIC*
Normal	ap	3 hrs	0.2442	0.0551	238740	825830	825860	6	6	6	6
Lognormal	ap	3 hrs	0.0542	0.0028	238740	425370	425390	3	2	1	1
Weibull	ap	3 hrs	0.1	0.0137	238740	493340	493360	4	5	5	5
Burr	ap	3 hrs	0.0376	0.0013	238740	425740	425770	1	1	2	2
Gamma	ap	3 hrs	0.1048	0.0124	238740	485750	485770	5	4	4	4
LogLogistic	ap	3 hrs	0.0417	0.003	238740	430880	430900	2	3	3	3
Rician	ap	3 hrs	0.4182	0.0686	238740	853850	853870	7	7	7	7
Normal	ap	1 dy	0.1845	0.0442	30878	88803	88820	6	6	7	7
Lognormal	ap	1 dy	0.0195	0.0007	30878	53177	53194	1	1	1	1
Weibull	ap	1 dy	0.0803	0.0131	30878	59783	59800	5	5	5	5
Burr	ap	1 dy	0.0197	0.0011	30878	53471	53496	2	2	2	2
Gamma	ap	1 dy	0.0738	0.0086	30878	57696	57713	4	4	4	4
LogLogistic	ap	1 dy	0.0214	0.0015	30878	53524	53541	3	3	3	3
Rician	ap	1 dy	0.2998	0.0471	30878	83383	83400	7	7	6	6
Normal	ap	7 dy	0.1167	0.033	4413	7529.9	7542.7	7	7	7	7
Lognormal	ap	7 dy	0.0176	0.0013	4413	5312.1	5324.9	1	1	1	1
Weibull	ap	7 dy	0.0786	0.0187	4413	6308.8	6321.6	5	6	5	5
Burr	ap	7 dy	0.0273	0.0032	4413	5411.2	5430.4	3	2	2	3
Gamma	ap	7 dy	0.0508	0.0066	4413	5653.6	5666.4	4	4	4	4
LogLogistic	ap	7 dy	0.0265	0.0034	4413	5416	5428.8	2	3	3	2
Rician	ap	7 dy	0.0861	0.0182	4413	6335.4	6348.1	6	5	6	6
Normal	ap	27 dy	0.0787	0.0235	1144	580.2	590.3	7	6	6	6
Lognormal	ap	27 dy	0.0184	0.0042	1144	408.3	418.4	1	1	1	1
Weibull	ap	27 dy	0.0754	0.0283	1144	606.8	616.9	5	7	7	7
Burr	ap	27 dy	0.0227	0.0053	1144	430.7	445.8	3	2	3	4
Gamma	ap	27 dy	0.0385	0.007	1144	430.7	440.8	4	4	3	3
LogLogistic	ap	27 dy	0.0226	0.0053	1144	428.7	438.8	2	2	2	2
Rician	ap	27 dy	0.0757	0.0222	1144	566.8	576.9	6	5	5	5
Normal	ap	0.5 yr	0.047	0.0276	169	-221.39	-215.135	3	4	3	3
Lognormal	ap	0.5 yr	0.0505	0.0237	169	-220.36	-214.096	4	2	4	4
Weibull	ap	0.5 yr	0.0668	0.0529	169	-212.17	-205.911	7	7	7	6
Burr	ap	0.5 yr	0.0545	0.039	169	-214.1	-204.711	6	5	5	7
Gamma	ap	0.5 yr	0.0466	0.0235	169	-221.41	-215.152	1	1	2	2
LogLogistic	ap	0.5 yr	0.0536	0.0411	169	-212.44	-206.178	5	6	6	5
Rician	ap	0.5 yr	0.0469	0.0275	169	-221.41	-215.152	2	3	1	1
Normal	ap	1 yr	0.1236	0.0476	84	-460.43	-455.569	3	3	4	4
Lognormal	ap	1 yr	0.1244	0.0456	84	-459.02	-454.156	6	1	6	6
Weibull	ap	1 yr	0.164	0.4733	84	-450.77	-445.908	7	7	7	7
Burr	ap	1 yr	0.0781	0.1023	84	-476.6	-469.31	1	5	2	2
Gamma	ap	1 yr	0.1241	0.0459	84	-459.51	-454.649	5	2	5	5
LogLogistic	ap	1 yr	0.081	0.1266	84	-478.4	-473.537	2	6	1	1
Rician	ap	1 yr	0.1236	0.0476	84	-460.44	-455.575	3	3	3	3

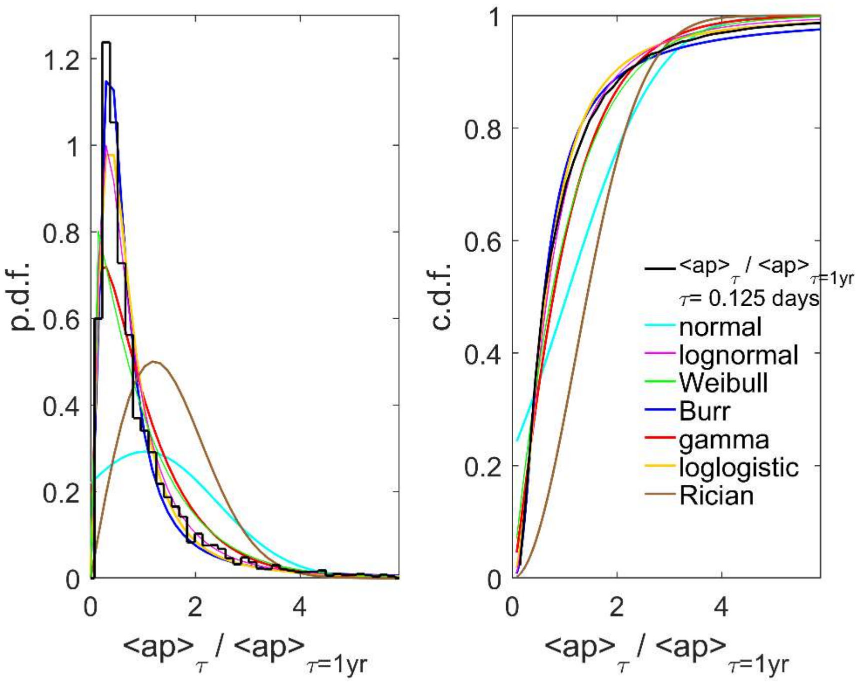

Figure S1. Best-fit distributions (in colours) fitted using the MLE method to the observed distributions (in black) for 7 tested distribution forms fitted to that for the ratio $<ap>_{\tau}/<ap>_{\tau=1yr}$ of the *ap* geomagnetic index data and an averaging timescale τ = 3hours. The plot on the right shows the probability distribution functions (pdfs) and on the left the corresponding cumulative distribution functions (cdfs). The fitted distributions are: (cyan) the normal (Gaussian) distribution; (mauve) the Lognormal distribution ; (green) the Weibull distribution ; (blue) the Burr distribution; (red) the Gamma distribution ; (orange) the LogLogistic distribution; and (brown) the Rician distribution. The optimum distribution parameters are given in Table S1 and the goodness-of fit metrics in Table S2.

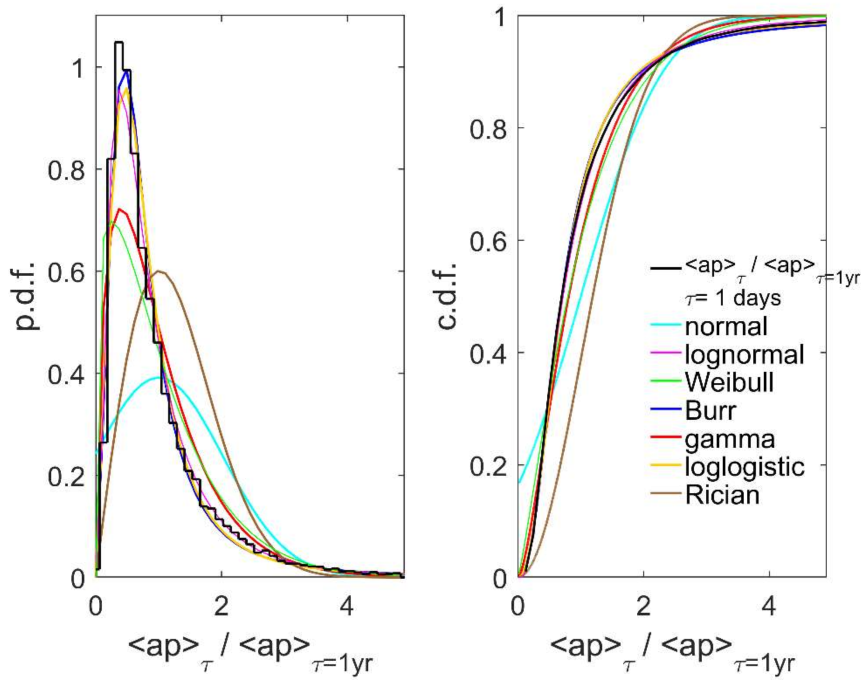

Figure S2. Same as Figure S1 but for an averaging timescale τ = 1 day.

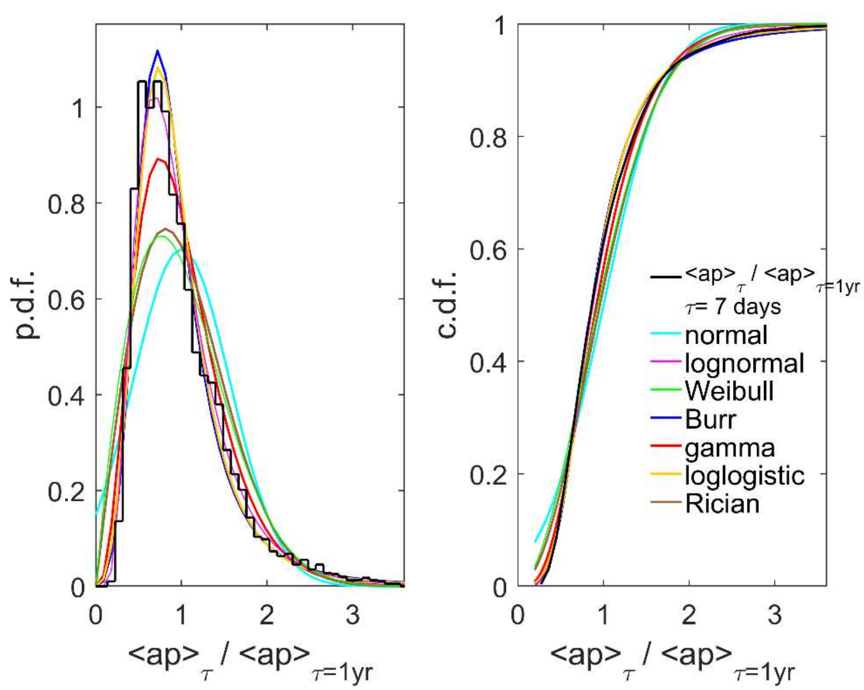

Figure S3. Same as Figure S1 but for an averaging timescale τ = 7 days.

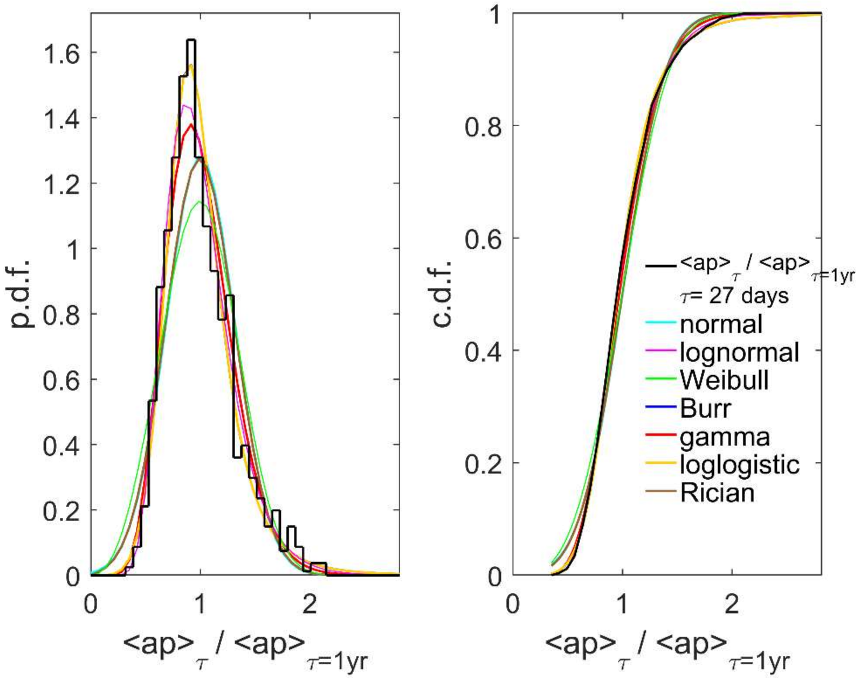

Figure S4. Same as Figure S1 but for an averaging timescale τ = 27 days.

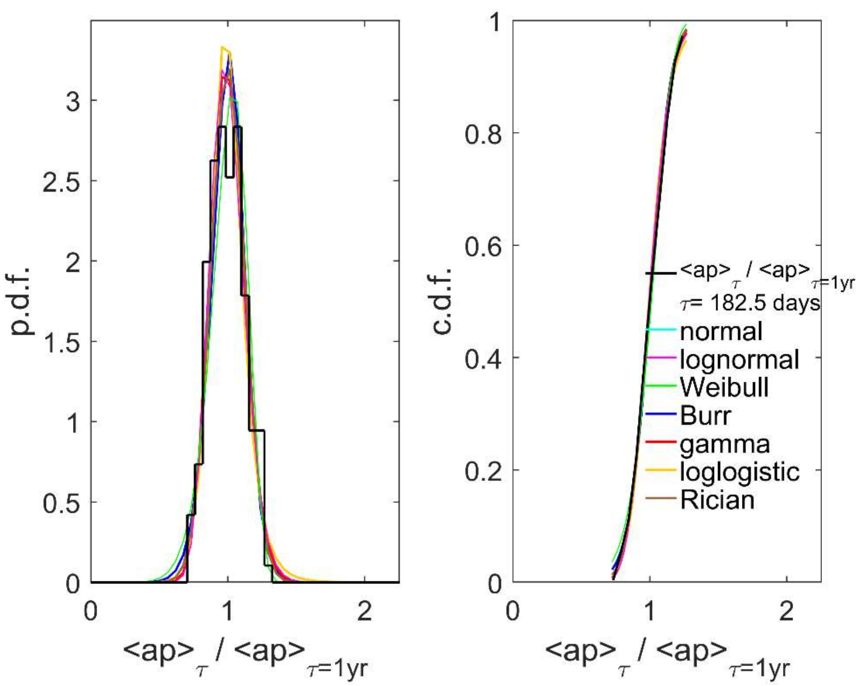

Figure S5. Same as Figure S1 but for an averaging timescale τ = 0.5 year

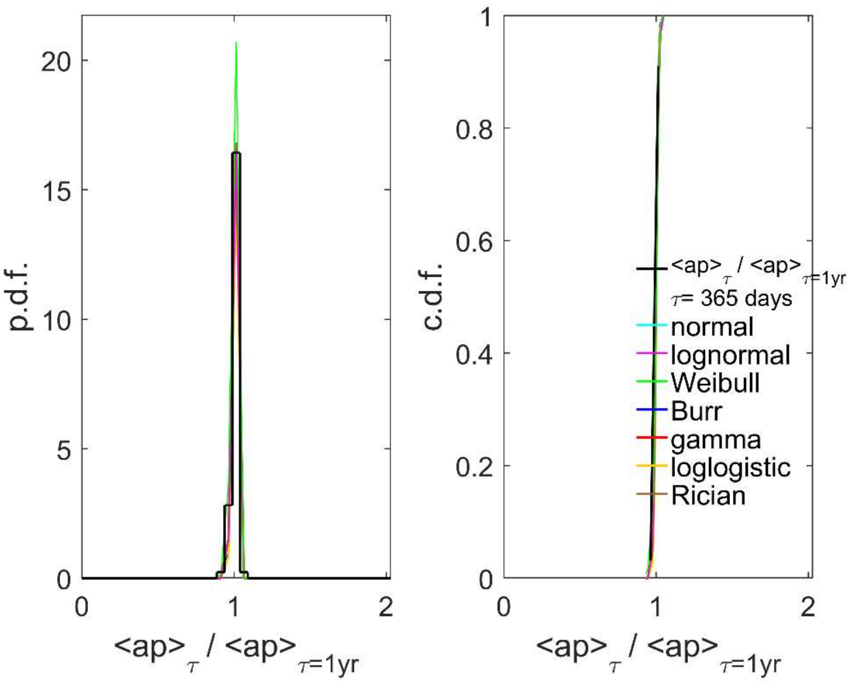

Figure S6. Same as Figure S1 but for an averaging timescale τ = 1 year

Table S3. Same Table S1 for the ratio *<Dst'>*$_\tau$*/<Dst>*$_{\tau=1yr}$ of the *Dst* geomagnetic index data

1	2	3	4	5	6	7	8	9	10	11	12
distribution		**Time scale**	**best**	**min**	**max**	**Best**	**Min**	**max**	**best**	**min**	**Max**
		τ	***A***	***A***	***A***	***B***	***B***	***B***	***C***	***C***	***C***
Normal	Dst	3 hrs	1.5118	1.5035	1.5202	1.572	1.5662	1.578			
Lognormal	Dst	3 hrs	-0.0419	-0.0475	-0.0363	1.0593	1.0554	1.0633			
Weibull	Dst	3 hrs	1.5691	1.5611	1.5771	1.0963	1.092	1.1006			
Burr	Dst	3 hrs	3.0954	2.9863	3.2085	1.3531	1.3438	1.3624	3.2124	3.1020	3.3267
Gamma	Dst	3 hrs	1.2385	1.2302	1.2469	1.2207	1.2107	1.2308			
LogLogistic	Dst	3 hrs	0.0332	0.0279	0.0385	0.5779	0.5753	0.5804			
Rician	Dst	3 hrs	0.0347	0	0.1591	1.5421	1.5378	1.5464			
Normal	Dst	1 dy	1.4063	1.386	1.4266	1.3758	1.3616	1.3903			
Lognormal	Dst	1 dy	-0.1276	-0.1478	-0.1074	1.3694	1.3553	1.3839			
Weibull	Dst	1 dy	1.4617	1.4413	1.4823	1.1063	1.0941	1.1187			
Burr	Dst	1 dy	4.9434	4.2892	5.6973	1.2574	1.2345	1.2807	5.3459	4.6628	6.1292
Gamma	Dst	1 dy	1.2064	1.1841	1.2291	1.1657	1.1392	1.1928			
LogLogistic	Dst	1 dy	-0.0208	-0.0359	-0.0058	0.5947	0.5873	0.6021			
Rician	Dst	1 dy	0.0413	0	0.3315	1.3909	1.3798	1.402			
Normal	Dst	7 dy	1.1984	1.1635	1.2332	0.9355	0.9117	0.961			
Lognormal	Dst	7 dy	-0.1578	-0.1931	-0.1226	0.9467	0.9226	0.9725			
Weibull	Dst	7 dy	1.305	1.2671	1.344	1.3322	1.295	1.3705			
Burr	Dst	7 dy	4.8309	3.2547	7.1703	1.4569	1.392	1.5249	7.4556	4.7048	11.8145
Gamma	Dst	7 dy	1.6224	1.5461	1.7025	0.7386	0.6981	0.7815			
LogLogistic	Dst	7 dy	-0.0718	-0.1041	-0.0395	0.5037	0.4882	0.5197			
Rician	Dst	7 dy	0.0302	0	1.0098	1.0748	1.0508	1.0994			
Normal	Dst	27 dy	1.0871	1.0427	1.1315	0.6238	0.5944	0.6572			
Lognormal	Dst	27 dy	-0.1219	-0.1759	-0.0678	0.76	0.7241	0.8007			
Weibull	Dst	27 dy	1.2192	1.1694	1.2711	1.7893	1.6951	1.8888			
Burr	Dst	27 dy	3.4811	1.8829	6.4359	1.9387	1.7762	2.1162	8.3695	3.1918	21.9464
Gamma	Dst	27 dy	2.5892	2.3555	2.8461	0.4199	0.3782	0.466			
LogLogistic	Dst	27 dy	-0.0478	-0.0934	-0.0022	0.3757	0.3539	0.3989			
Rician	Dst	27 dy	0.0449	0	1.9464	0.8857	0.83	0.9452			
Normal	Dst	0.5 yr	1.0098	0.9519	1.0676	0.3173	0.2826	0.3652			
Lognormal	Dst	0.5 yr	-0.0538	-0.1273	0.0197	0.4033	0.3592	0.4641			
Weibull	Dst	0.5 yr	1.1185	1.0564	1.1842	3.3126	2.9054	3.7767			
Burr	Dst	0.5 yr	1.3608	0.9812	1.8874	4.2419	3.38	5.3237	3.0008	1.1209	8.0339
Gamma	Dst	0.5 yr	8.0391	6.2672	10.3121	0.1256	0.0971	0.1624			
LogLogistic	Dst	0.5 yr	-0.0146	-0.0705	0.0412	0.185	0.1586	0.2158			
Rician	Dst	0.5 yr	0.9507	0.887	1.0144	0.3289	0.2865	0.3776			
Normal	Dst	1 yr	1	0.9946	1.0054	0.0206	0.0176	0.0254			
Lognormal	Dst	1 yr	-0.0002	-0.0056	0.0052	0.0207	0.0177	0.0255			
Weibull	Dst	1 yr	1.01	1.0044	1.0156	48.4687	40.6213	57.8321			
Burr	Dst	1 yr	1.0003	0.9859	1.015	0.0906	62.5014	0.0001	1.0203	0.4363	2.3863
Gamma	Dst	1 yr	2338.8	1635.3	3344.9	0.0004	0.0003	0.0006			
LogLogistic	Dst	1 yr	0	-0.0047	0.0048	0.011	0.0088	0.0136			
Rician	Dst	1 yr	0.9998	0.9946	1.005	0.0206	0.0173	0.0247			

Table S4. Same Table S2 for the ratio $<Dst'>_{\tau}/<Dst>_{\tau=1yr}$ of the *Dst* geomagnetic index data

1	2	3	4	5	6	7	8	9	10	11	12
distribution		Time	Goodness of fit tests					Rank			
		τ	*D*	D_{MS}	*N*	*AIC*	*BIC*	*D*	Δ_{MS}	*AIC*	*BIC*
Normal	Dst	3 hrs	0.1698	0.0114	136380	510440	510460	6	6	6	6
Lognormal	Dst	3 hrs	0.0658	0.0036	136380	391340	391360	5	5	5	5
Weibull	Dst	3 hrs	0.0363	0.0015	136380	383510	383530	4	3	3	3
Burr	Dst	3 hrs	0.0137	0.001	136380	377930	377960	1	1	1	1
Gamma	Dst	3 hrs	0.0319	0.0012	136380	381850	381870	3	2	2	2
LogLogistic	Dst	3 hrs	0.0309	0.0018	136380	385830	385850	2	4	4	4
Rician	Dst	3 hrs	0.2779	0.0161	136380	520540	520560	7	7	7	7
Normal	Dst	1 dy	0.1533	0.0114	17664	61402	61418	6	6	6	6
Lognormal	Dst	1 dy	0.1066	0.0094	17664	56729	56745	5	5	5	5
Weibull	Dst	1 dy	0.0311	0.002	17664	47077	47093	3	3	3	3
Burr	Dst	1 dy	0.0213	0.0016	17664	46777	46800	1	1	1	1
Gamma	Dst	1 dy	0.0271	0.0019	17664	47009	47024	2	2	2	2
LogLogistic	Dst	1 dy	0.0416	0.0026	17664	48436	48452	4	4	4	4
Rician	Dst	1 dy	0.2514	0.0164	17664	63165	63181	7	7	7	7
Normal	Dst	7 dy	0.1015	0.0112	2772	7501	7512.8	6	6	7	7
Lognormal	Dst	7 dy	0.0799	0.0079	2772	6692	6703.8	5	5	5	5
Weibull	Dst	7 dy	0.0241	0.0015	2772	6214.5	6226.3	2	2	3	3
Burr	Dst	7 dy	0.0183	0.0012	2772	6191.2	6209	1	1	1	1
Gamma	Dst	7 dy	0.0275	0.0017	2772	6211	6222.8	3	3	2	2
LogLogistic	Dst	7 dy	0.0456	0.0037	2772	6474	6485.8	4	4	4	4
Rician	Dst	7 dy	0.1609	0.0126	2772	7225	7236.8	7	7	6	6
Normal	Dst	27 dy	0.07	0.0085	763	1449.1	1458.3	6	6	6	6
Lognormal	Dst	27 dy	0.0886	0.0168	763	1564.5	1573.7	7	7	7	7
Weibull	Dst	27 dy	0.0366	0.0047	763	1330.1	1339.3	2	3	2	1
Burr	Dst	27 dy	0.0283	0.0038	763	1326.8	1340.7	1	2	1	2
Gamma	Dst	27 dy	0.0431	0.0059	763	1354.8	1364	3	4	4	4
LogLogistic	Dst	27 dy	0.0515	0.0063	763	1411.5	1420.8	5	5	5	5
Rician	Dst	27 dy	0.0439	0.0037	763	1347.4	1356.7	4	1	3	3
Normal	Dst	0.5 yr	0.0877	0.0432	119	68.4819	74.0401	4	3	1	1
Lognormal	Dst	0.5 yr	0.1461	0.0841	119	112.767	118.325	7	7	7	7
Weibull	Dst	0.5 yr	0.0986	0.0545	119	74.82	80.3782	5	5	4	4
Burr	Dst	0.5 yr	0.0695	0.0374	119	70.4156	78.7529	1	2	3	3
Gamma	Dst	0.5 yr	0.112	0.0595	119	85.804	91.3623	6	6	6	6
LogLogistic	Dst	0.5 yr	0.0817	0.0369	119	77.0085	82.5667	2	1	5	5
Rician	Dst	0.5 yr	0.0876	0.0437	119	68.6028	74.161	3	4	2	2
Normal	Dst	1 yr	0.0746	0.0167	60	-291.41	-287.226	5	1	4	4
Lognormal	Dst	1 yr	0.0709	0.0238	60	-291.04	-286.854	3	4	6	6
Weibull	Dst	1 yr	0.1267	0.2017	60	-282.64	-278.448	7	7	7	7
Burr	Dst	1 yr	0.0658	0.1232	60	-293.54	-287.257	2	5	2	2
Gamma	Dst	1 yr	0.0721	0.0211	60	-291.19	-286.999	4	3	5	5
LogLogistic	Dst	1 yr	0.0653	0.128	60	-295.54	-291.349	1	6	1	1
Rician	Dst	1 yr	0.0746	0.0167	60	-291.42	-287.235	5	1	3	3

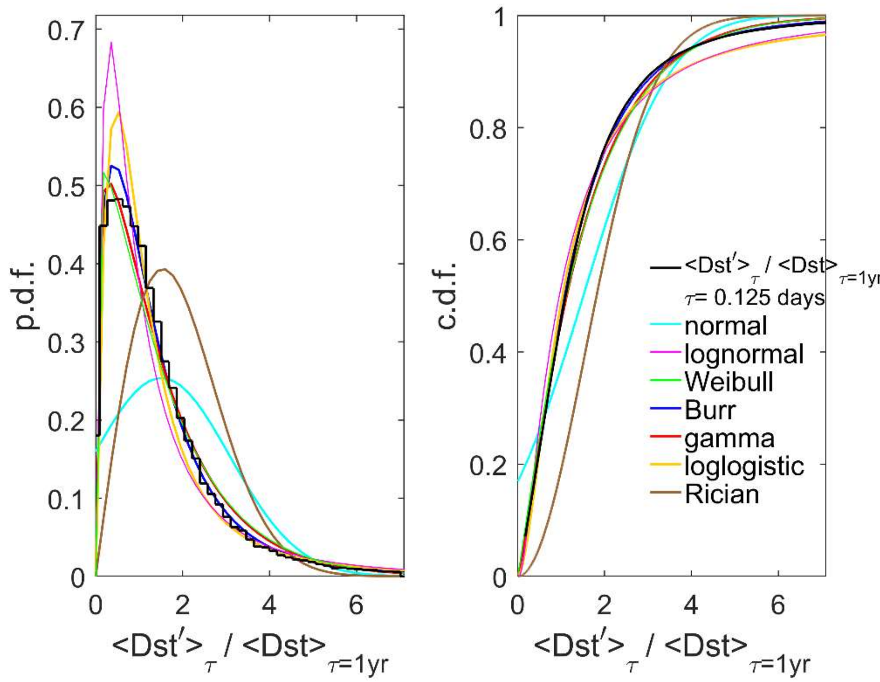

Figure S7. Same as Figure S1 but for for the ratio $<Dst>_{\tau}/<Dst>_{\tau=1yr}$ of the *ap* geomagnetic index data (and for an averaging timescale τ = 3 hours)

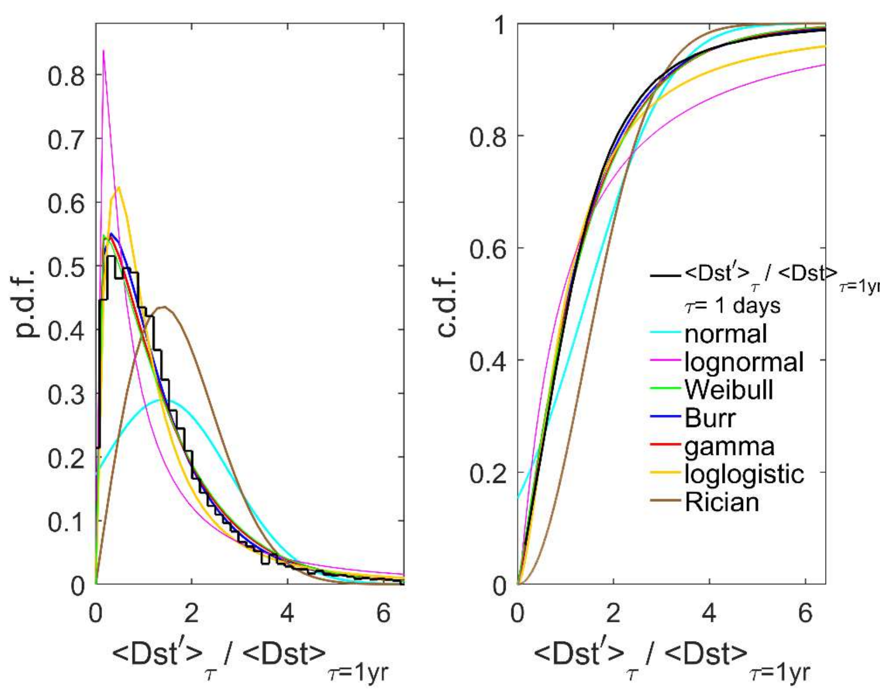

Figure S8. Same as Figure S7 but for for an averaging timescale τ = 1 day.

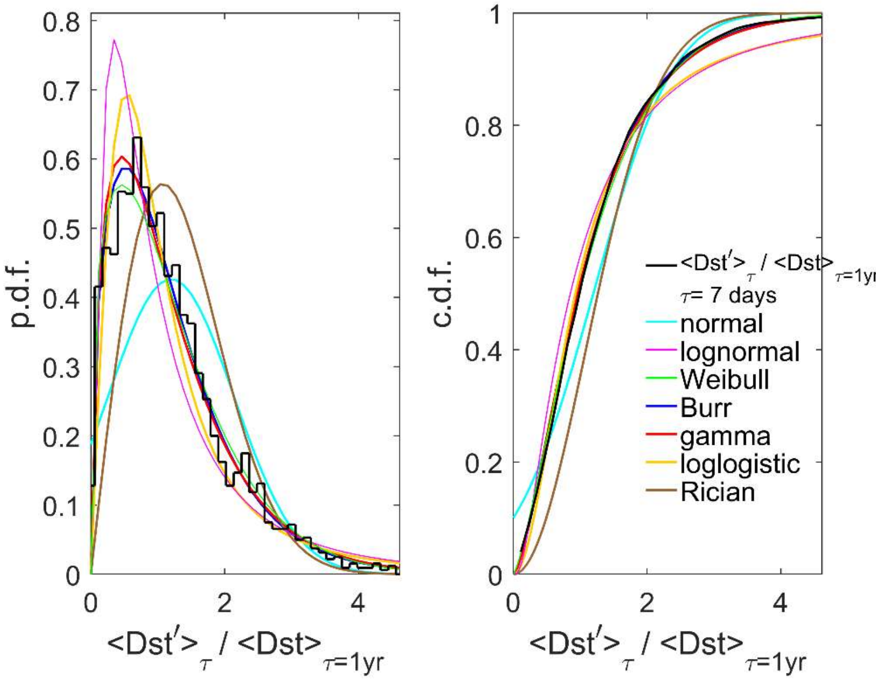

Figure S9. Same as Figure S7 but for for an averaging timescale τ = 7 days.

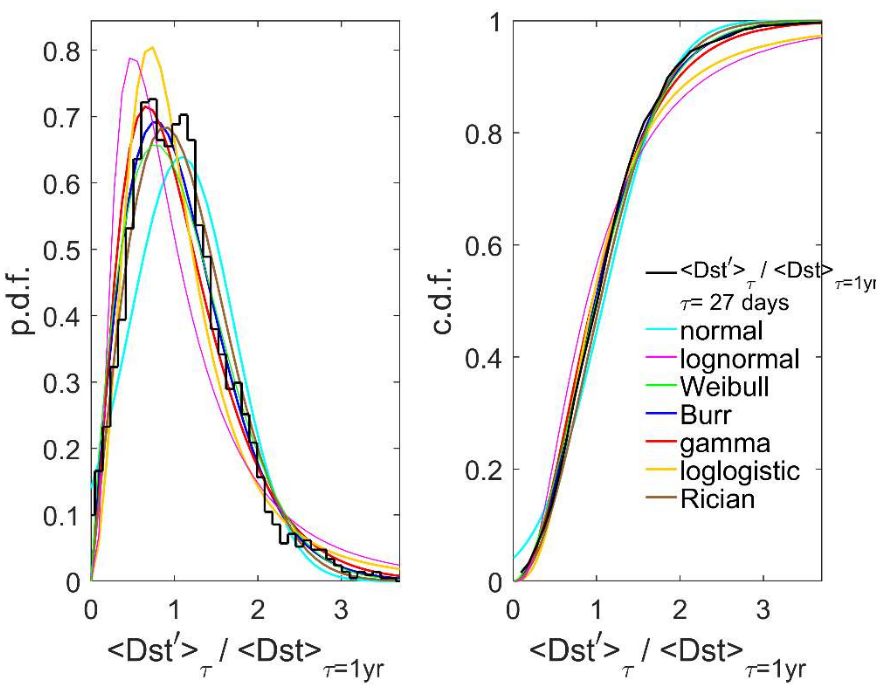

Figure S10. Same as Figure S7 but for for an averaging timescale τ = 27 days.

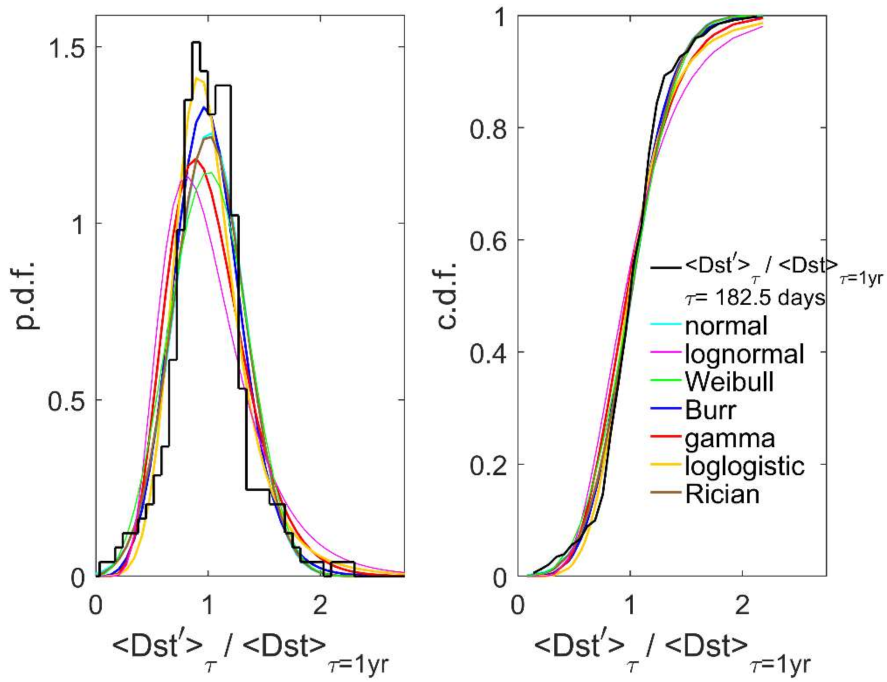

Figure S11. Same as Figure S7 but for for an averaging timescale τ = 0.5 year.

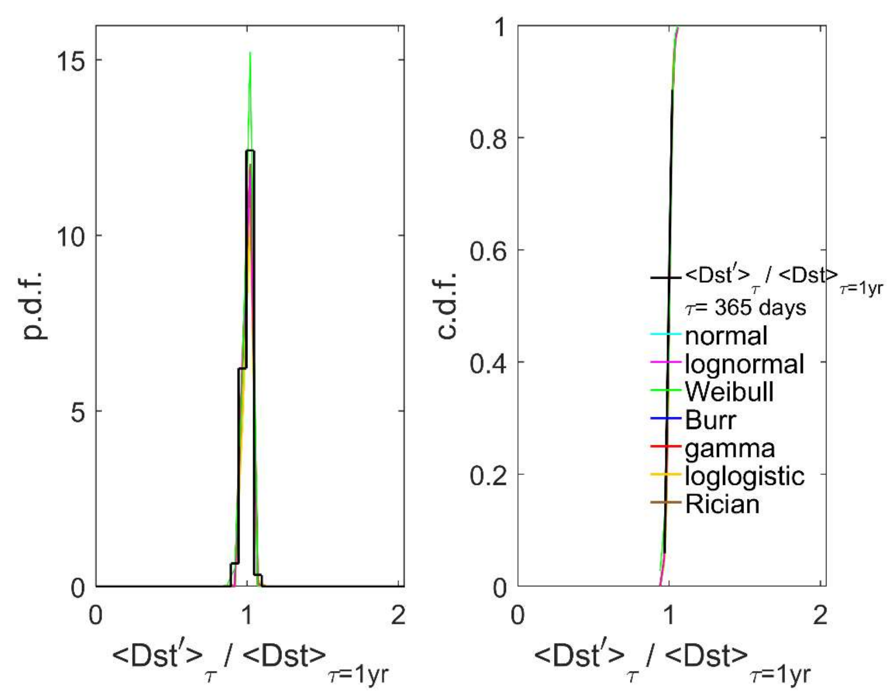

Figure S12. Same as Figure S7 but for for an averaging timescale τ = 1 year.

Table S5. Same Table S1 for the ratio $<P_\alpha>_\tau/<P_\alpha>_{\tau=1yr}$ for the estimated power input into the magnetosphere, P_α

1	2	3	4	5	6	7	8	9	10	11	12
distribution		**Time**	**best**	**min**	**max**	**best**	**min**	**max**	**best**	**min**	**Max**
		τ	***A***	***A***	***A***	***B***	***B***	***B***	***C***	***C***	***C***
Normal	P_a	3 hrs	1	0.99	1.01	1.2135	1.2064	1.2206			
Lognormal	P_a	3 hrs	-0.607	-0.618	-0.5959	1.3353	1.3275	1.3431			
Weibull	P_a	3 hrs	0.9806	0.9718	0.9896	0.9586	0.9527	0.9646			
Burr	P_a	3 hrs	5.4574	4.9261	6.046	1.0647	1.0545	1.075	6.9359	6.3622	7.5613
Gamma	P_a	3 hrs	0.9561	0.9463	0.9659	1.046	1.0321	1.06			
LogLogistic	P_a	3 hrs	-0.4768	-0.4867	-0.4669	0.6968	0.692	0.7017			
Rician	P_a	3 hrs	0.0163	0	0.1282	1.1118	1.1072	1.1165			
Normal	P_a	1 dy	1	0.9806	1.0194	0.8626	0.8492	0.8766			
Lognormal	P_a	1 dy	-0.2885	-0.3064	-0.2705	0.7999	0.7874	0.8128			
Weibull	P_a	1 dy	1.0967	1.0774	1.1163	1.3368	1.3158	1.3582			
Burr	P_a	1 dy	1.1486	1.0567	1.2485	1.9523	1.891	2.0156	1.7629	1.5808	1.966
Gamma	P_a	1 dy	1.8827	1.8283	1.9388	0.5312	0.5136	0.5493			
LogLogistic	P_a	1 dy	-0.2601	-0.2772	-0.243	0.4384	0.4303	0.4467			
Rician	P_a	1 dy	0.012	0	0.6305	0.9338	0.9227	0.9451			
Normal	P_a	7 dy	1	0.9738	1.0262	0.4416	0.424	0.4611			
Lognormal	P_a	7 dy	-0.0882	-0.113	-0.0634	0.4181	0.4015	0.4366			
Weibull	P_a	7 dy	1.1302	1.1006	1.1605	2.3746	2.2768	2.4767			
Burr	P_a	7 dy	0.9182	0.8336	1.0114	4.1464	3.7502	4.5845	1.0157	0.7889	1.3077
Gamma	P_a	7 dy	5.8285	5.3724	6.3232	0.1716	0.1576	0.1868			
LogLogistic	P_a	7 dy	-0.0911	-0.1159	-0.0662	0.2399	0.2284	0.2519			
Rician	P_a	7 dy	0.8011	0.7424	0.8599	0.5259	0.4865	0.5686			
Normal	P_a	27 dy	1	0.9728	1.0272	0.2321	0.2148	0.2534			
Lognormal	P_a	27 dy	-0.0262	-0.0529	0.0006	0.2285	0.2115	0.2494			
Weibull	P_a	27 dy	1.0926	1.0624	1.1237	4.3949	4.0438	4.7764			
Burr	P_a	27 dy	0.976	0.8796	1.0831	7.6117	6.2341	9.2939	1.0163	0.6164	1.6756
Gamma	P_a	27 dy	19.2766	16.376	22.6909	0.0519	0.044	0.0612			
LogLogistic	P_a	27 dy	-0.0275	-0.0541	-0.001	0.1306	0.1186	0.1439			
Rician	P_a	27 dy	0.9709	0.9426	0.9992	0.2358	0.2166	0.2568			
Normal	P_a	0.5 yr	1	0.9736	1.0264	0.0838	0.0697	0.1081			
Lognormal	P_a	0.5 yr	-0.0036	-0.0303	0.0232	0.0848	0.0706	0.1094			
Weibull	P_a	0.5 yr	1.0383	1.0127	1.0646	12.8352	10.2692	16.0424			
Burr	P_a	0.5 yr	1.0548	0.9075	1.226	17.2865	10.986	27.2004	1.9909	0.3422	11.5837
Gamma	P_a	0.5 yr	140.567	91.6971	215.4817	0.0071	0.0046	0.0109			
LogLogistic	P_a	0.5 yr	-0.0011	-0.0266	0.0244	0.0483	0.0376	0.062			
Rician	P_a	0.5 yr	0.9965	0.971	1.0219	0.0839	0.0677	0.104			
Normal	P_a	1 yr	1	0.9978	1.0022	0.0047	0.0037	0.007			
Lognormal	P_a	1 yr	0	-0.0022	0.0022	0.0047	0.0037	0.007			
Weibull	P_a	1 yr	1.0021	1.0004	1.0038	263.7103	190.3309	365.38			
Burr	P_a	1 yr	1.0044	0.9855	1.0237	0.3204	139.1549	0.0007	2.7958	0.0388	201.2463
Gamma	P_a	1 yr	44.9673	24.559	82.3346	0	0	0			
LogLogistic	P_a	1 yr	0.0002	-0.0015	0.002	0.0024	0.0017	0.0034			
Rician	P_a	1 yr	1	0.998	1.002	0.0047	0.0035	0.0064			

Table S6. Same Table S2 for the ratio $<P_\alpha>_\tau/<P_\alpha>_{\tau=1yr}$ for the estimated power input into the magnetosphere, P_α

1	2	3	4	5	6	7	8	9	10	11	12
distribution		Time	Goodness of fit tests					Rank			
		τ	*D*	D_{MS}	*N*	*AIC*	*BIC*	*D*	Δ_{MS}	*AIC*	*BIC*
Normal	P_a	3 hrs	0.2049	0.0285	56130	181010	181020	6	5	6	6
Lognormal	P_a	3 hrs	0.0869	0.0163	56130	123610	123630	5	4	5	5
Weibull	P_a	3 hrs	0.0226	0.0099	56130	112080	112100	3	3	2	2
Burr	P_a	3 hrs	0.019	0.007	56130	111230	111260	1	1	1	1
Gamma	P_a	3 hrs	0.0216	1.0105	56130	112190	112200	2	7	3	3
LogLogistic	P_a	3 hrs	0.0488	0.0094	56130	117490	117510	4	2	4	4
Rician	P_a	3 hrs	0.3321	0.0474	56130	204200	204220	7	6	7	7
Normal	P_a	1 dy	0.1386	0.0272	7632	19407	19421	6	7	7	7
Lognormal	P_a	1 dy	0.0341	0.002	7632	13851	13865	3	3	4	4
Weibull	P_a	1 dy	0.0536	0.0062	7632	14203	14217	5	5	5	5
Burr	P_a	1 dy	0.0097	0.0006	7632	13386	13407	1	1	1	1
Gamma	P_a	1 dy	0.038	0.0023	7632	13759	13772	4	4	3	3
LogLogistic	P_a	1 dy	0.02	0.001	7632	13514	13528	2	2	2	2
Rician	P_a	1 dy	0.202	0.0236	7632	17582	17596	7	6	6	6
Normal	P_a	7 dy	0.0951	0.0253	1095	1321.5	1331.5	7	7	7	7
Lognormal	P_a	7 dy	0.0146	0.0019	1095	1008.6	1018.6	1	1	1	1
Weibull	P_a	7 dy	0.0691	0.0183	1095	1202	1212	5	5	5	5
Burr	P_a	7 dy	0.0197	0.0035	1095	1036.6	1051.6	2	2	3	3
Gamma	P_a	7 dy	0.0433	0.0049	1095	1050.5	1060.5	4	4	4	4
LogLogistic	P_a	7 dy	0.0202	0.0035	1095	1034.6	1044.6	3	2	2	2
Rician	P_a	7 dy	0.0792	0.0216	1095	1240	1250	6	6	6	6
Normal	P_a	27 dy	0.0637	0.0272	284	-19.697	-12.3991	6	6	6	6
Lognormal	P_a	27 dy	0.0267	0.0118	284	-43.444	-36.1462	1	1	1	1
Weibull	P_a	27 dy	0.0809	0.0435	284	2.6857	9.9836	7	7	7	7
Burr	P_a	27 dy	0.0358	0.0133	284	-35.796	-24.8487	3	3	4	4
Gamma	P_a	27 dy	0.0387	0.0141	284	-40.318	-33.0203	4	4	2	2
LogLogistic	P_a	27 dy	0.0355	0.0132	284	-37.792	-30.4936	2	2	3	3
Rician	P_a	27 dy	0.0628	0.0267	284	-20.619	-13.3213	5	5	5	5
Normal	P_a	0.5 yr	0.0531	0.0126	42	-85.106	-81.6303	4	1	2	2
Lognormal	P_a	0.5 yr	0.0452	0.0189	42	-84.37	-80.8949	1	4	4	4
Weibull	P_a	0.5 yr	0.0981	0.0404	42	-82.29	-78.8143	7	6	7	6
Burr	P_a	0.5 yr	0.0597	0.0257	42	-82.673	-77.4598	6	5	6	7
Gamma	P_a	0.5 yr	0.0456	0.0158	42	-84.727	-81.2521	2	3	3	3
LogLogistic	P_a	0.5 yr	0.0535	0.0415	42	-83.874	-80.3988	5	7	5	5
Rician	P_a	0.5 yr	0.053	0.0126	42	-85.117	-81.6418	3	1	1	1
Normal	P_a	1 yr	0.1299	46.2965	21	-161.45	-159.362	3	3	5	5
Lognormal	P_a	1 yr	0.1289	45.5454	21	-161.33	-159.237	1	1	7	7
Weibull	P_a	1 yr	0.1934	116.519	21	-164.68	-162.589	7	7	1	1
Burr	P_a	1 yr	0.1756	85.2282	21	-162.9	-159.768	6	6	3	3
Gamma	P_a	1 yr	0.1292	45.795	21	-161.39	-159.303	2	2	6	6
LogLogistic	P_a	1 yr	0.1577	52.0844	21	-164.32	-162.234	5	5	2	2
Rician	P_a	1 yr	0.1299	46.2965	21	-161.48	-159.387	3	3	4	4

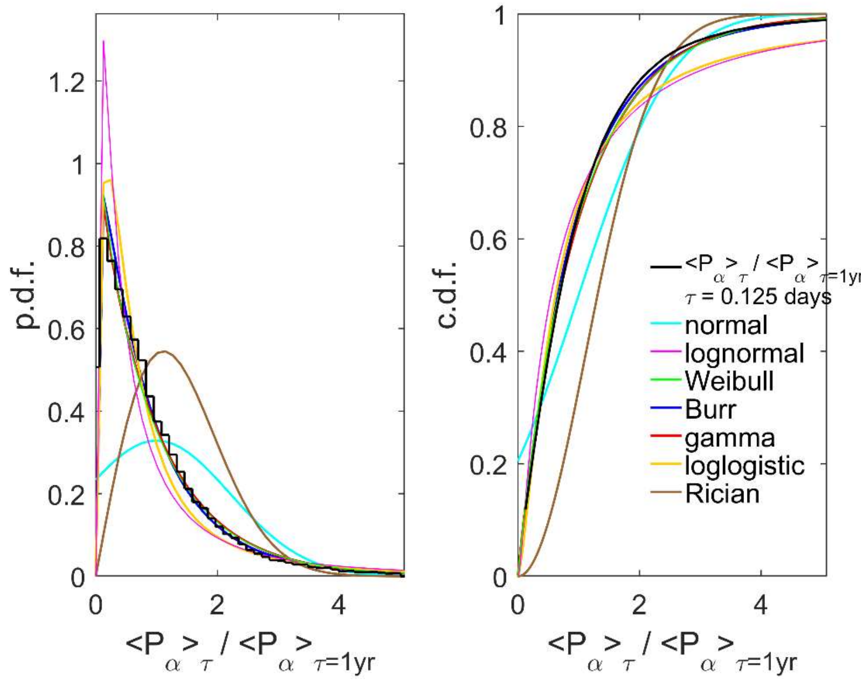

Figure S13. Same as Figure S1 but for for the ratio $\langle P_\alpha \rangle_\tau / \langle P_\alpha \rangle_{\tau=1yr}$ for the estimated power input into the magnetosphere, P_α (and for an averaging timescale τ = 3 hours)

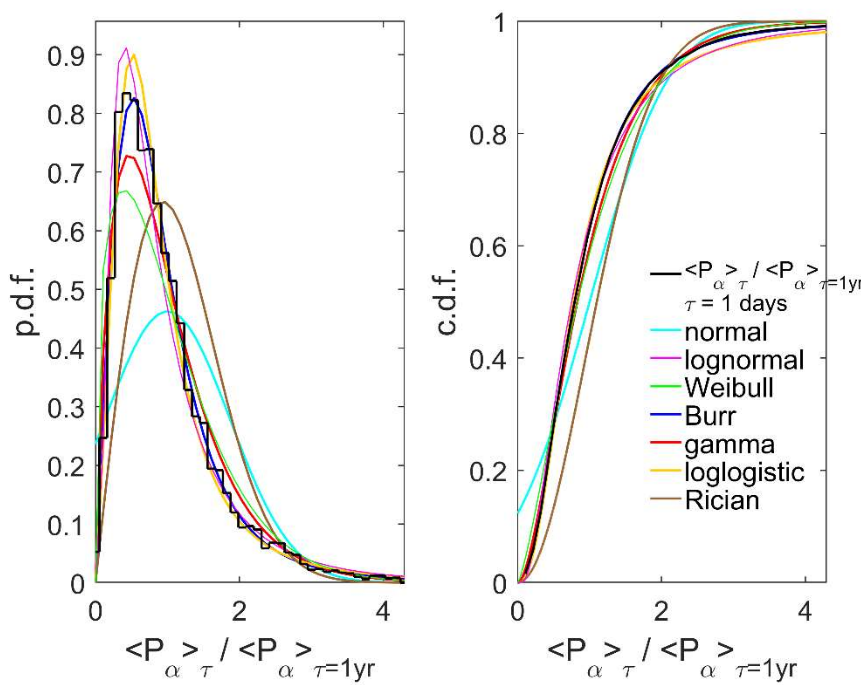

Figure S14. Same as Figure S13 but for for an averaging timescale τ = 1 day.

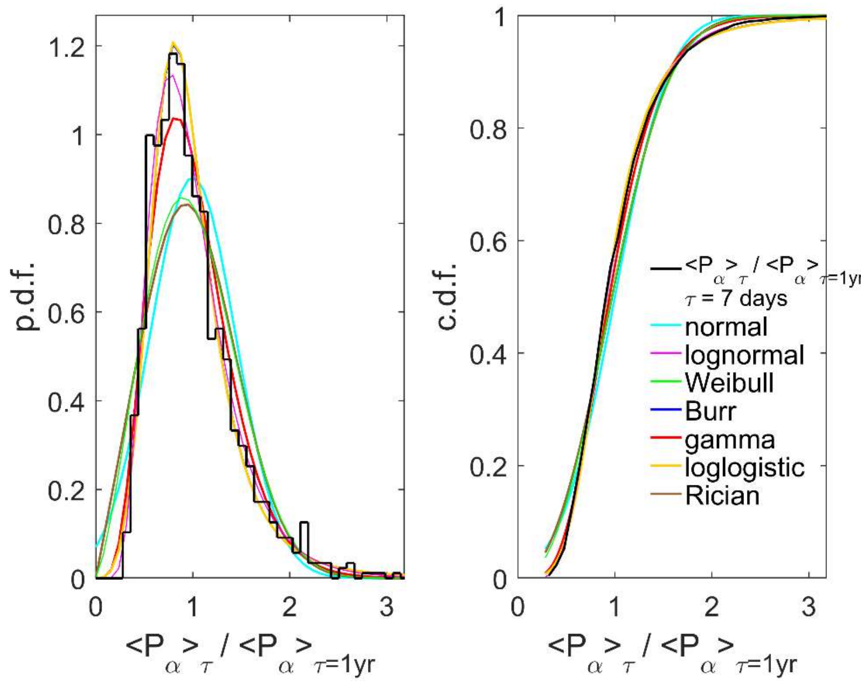

Figure S15. Same as Figure S13 but for for an averaging timescale τ = 7 days

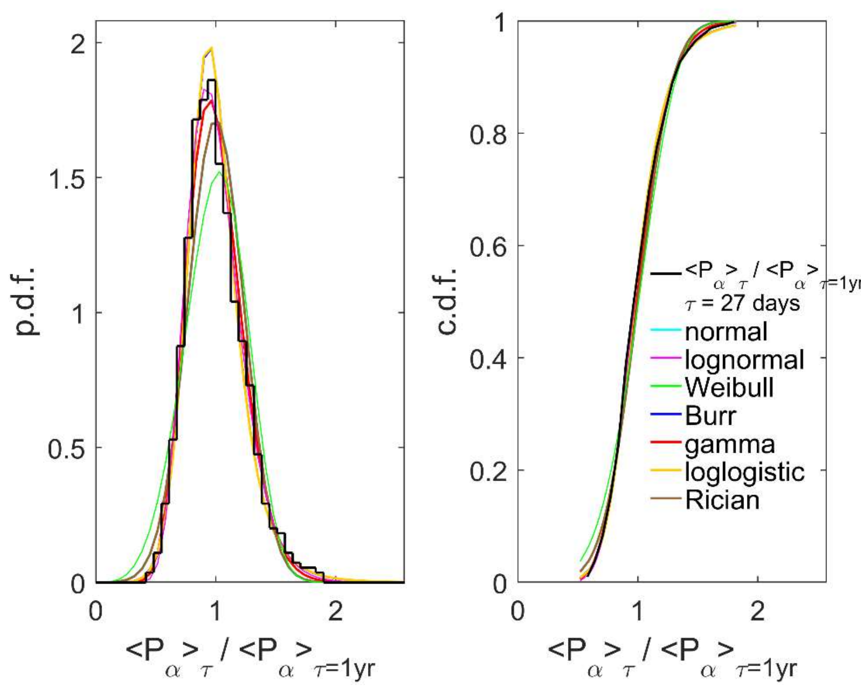

Figure S16. Same as Figure S13 but for for an averaging timescale τ = 27 days

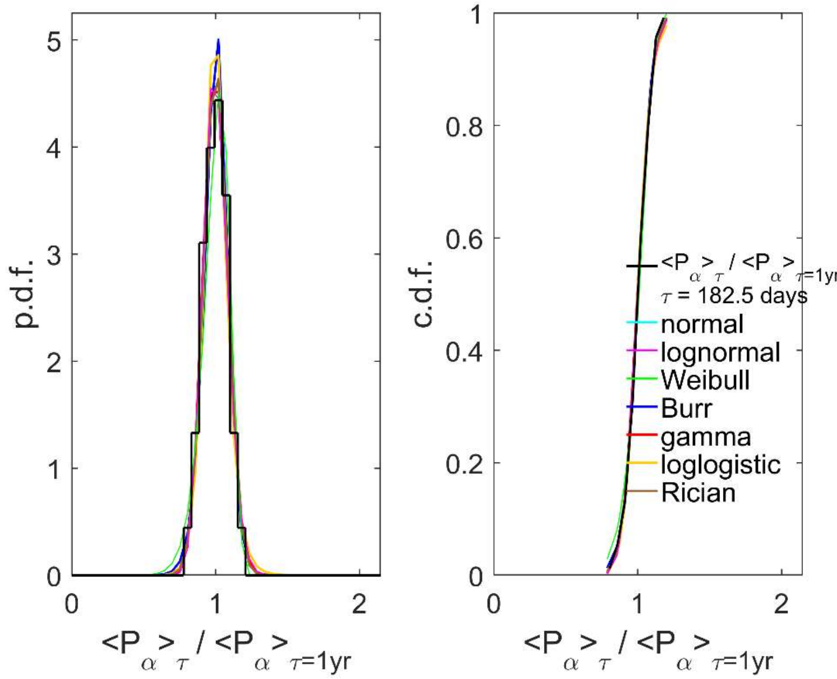

Figure S17. Same as Figure S13 but for for an averaging timescale τ = 0.5 year

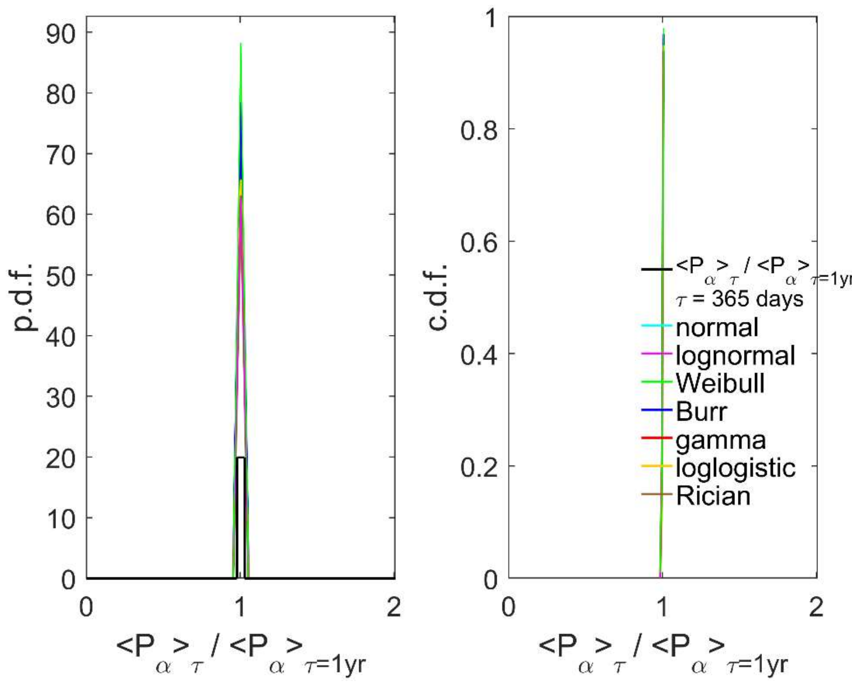

Figure S18. Same as Figure S13 but for for an averaging timescale τ = 1 year

Part 3. List of largest storms in rank order defined by 24-hour running means of corrected *ap* values, Ap_C*

As pointed out by *Allen* [1982], taking means over each calendar day is not appropriate when identifying a geomagnetic storm because any storm that straddles 24hrs UT would be recorded as two moderately-active days rather than a single storm. Hence, daily mean *ap* (i.e., *Ap*) values are not appropriate and we here employ Allen's idea of using 8-point running (boxcar) means over all 24-hour intervals, termed *Ap**, as has also used by *Kappenman* [2005] and *Cliver and Svalgaard* [2004].

However, we also make corrections to the *ap* values. Our recent research on the collective response of networks of stations contributing to geomagnetic indices has shown that the *ap* index tends, on average, to exaggerate the semi-annual variation in geomagnetic activity and has a low response in northern-hemisphere winter [Lockwood, M., A. Chambodut , I. D. Finch, L. A. Barnard , and M. J. Owens (2019) Time-of-day / time-of-year response functions of planetary geomagnetic indices, to be submitted to J. Space Weather Space Clim.]. Lockwood et al. [2018d, e] have made corrections to the *aa* geomagnetic index and our work on the response functions of the various mid-latitude range indices employs the model that was developed for that work. This research reveals that the *am* geomagnetic index has a very flat, almost ideal, time-of-day/time-of-year response at all activity levels because it employs relatively uniform rings of mid-latitude stations in both hemispheres and uses weighted means to account for any spatial non-uniformity of the station network. *Cliver and Svalgaard* [2004] recognized the quality of the *am* index, compared to indices derived from a less-ideal distribution of stations, and used it to correct for the false time-of-day variation in the *aa* index (and so created what they termed aa_m). However, they did not correct for the associated false time-of-year variation in *aa* [*Lockwood et al.,* 2018e]. They then used the *Allen* [1982] suggestion of 24-hour running means of aa_m (which they termed Aa_m*) which largely suppresses the false time-of-day variation anyway. We here apply the same philosophy that *Cliver and Svalgaard* [2004] adopted, but use *am* to correct for the false time-of-year variation in *ap*. We do this because the *am* index data only extends back to 1959 whereas the *ap* index is available from 1932 onward.

The *ap* index is compiled from a network of stations that is predominantly in the northern hemisphere, with many in Europe. The compilation of the *ap* index employs station- and activity-dependent "look-up tables" to convert the data from a station into a form that matches that from the Niemegk reference station before averaging them. Our research shows that this causes *ap* to slightly exaggerate the average semi-annual variation and gives a poorer response in northern-hemisphere winter compared to *am*. However, the effect is complex and depends on the level of geomagnetic activity. We here employ a corrected *ap* index, ap_C, which allows for these effects as a function of the fraction of each year (*F*) using the formula

$$ap_C(F) = ap(F) \times \underline{C}_{ap}(F,\mathrm{ap})$$

where $\underline{C}_{ap}(F,ap) = (\langle am(F,ap)\rangle_{bin} / \langle am\rangle_{all}) / (\langle ap(F,ap)\rangle_{bin} / \langle ap\rangle_{all})$

$$= (\langle am(F,ap)\rangle_{bin} / \langle ap(F,ap)\rangle_{bin}) \times (\langle ap\rangle_{all} / \langle am\rangle_{all})$$

where the subscript "all" refers to the averaging of all co-incident *ap* and *am* data for 1959-2017 (inclusive) and the subscript "bin" refers to the averaging of data in a given *F* and *ap* bin for the same interval. Multiplying by the ratio of the all-over means of *ap* and *am* means that we correct for the variation with *F* but do not change the average levels of *ap*. In practice, the data were divided into 40 percentiles of the overall *ap* distribution giving 6282 samples in each *ap* bin, the values of $C_{ap}(F,ap)$ were then fitted with a 6th order polynomial in *F*. Note that we are not concerned with any limitations in the UT dependence of the response of *ap* because we use averages over 24-hour intervals, Ap_C*. Further details are given in Appendix A of the main paper. We note that this correction is only approximate because the network of stations used to generate the *ap* index has changed a number of times since 1932. However, we do not find any major discontinuities in the derived $C_{ap}(F,ap)$ at any of these changes since 1959 and so use the assumption that effects of changes before this date also have negligible effect.

We then follow the procedure of *Allen* [1982] to make 24-hour boxcar means of ap_C, Ap_C*. For the purposes of identifying and ranking storm days we take the largest value of the 8 such running-means in each calendar day $[Ap_C*]_{MAX}$. The 100 largest values of $[Ap_C*]_{MAX}$ since 1932 are given in Table S7 in rank order. Although there are similarities, this list has a somewhat different ranking order to previous studies [e.g., *Nevanlinna et al.*, 2006; *Kappenman*, 2005; *Cliver and Svalgaard*, 2004], largely because we have made allowance for the variation of *ap* response with time of year. Note that even quite small changes in the estimated magnitude of the storm day can have a large effect on its ranking order.

In the table "est." means estimated rather than directly observed: these events (listed in italics) are not included in the rank order but are listed to act as context. The "estimate 2", $[Ap*]_{MAX}$ values are taken to be 296±16 for both the Carrington (03 September1859) and STEREO (23 July 2012) events and have not been subject to the same correction for time of year as the observed *ap* estimates. Also given are values for these events that have been corrected ("estimate 1", $[Ap_C*]_{MAX}$ values) of 224±12 and 221±12, which drops them both down the ranking order by several places). The rationale that this correction is required for these estimated event sizes is discussed in the main text. Note that all these values come from *Cliver and Svalgaard's* [2004] estimate of a peak of $Aa*$ = 425nT for the Carrington event and we do not here attempt to estimate, or employ, uncertainties on that estimate – we simply evaluate its consequences for the likely $Ap*$ and Ap_C* values.

Table S7. Storm days ranked by the largest value of the 8-point (1 day) boxcar smoothed mean in the day ($[Ap_C^*]_{MAX}$) of ap_C, the *ap* geomagnetic index that has been corrected to allow for its time-of year dependence. The value of $[Ap_C^*]_{MAX}$ as a ratio of the annual mean for the calendar year in question is also given for each storm day. The coloured symbols in column 1 are the same as used in Figure 2 of main text.

	Date	Sun-spot cycle	Cycle-phase (°)	Notes: event name, notable features, and references	$[Ap_C^*]_{MAX}$	$[Ap_C^*]_{MAX}$ / $<ap_C>_{1year}$
Est 2 ■	*03 September1859*	*9*	*104*	*Peak of "Carrington" event* [1,45,46,48]	*284±30*	*25.9±2.7*
Est 2. ■	*23 July 2012*	*24*	*133*	*STEREO-A event* [2]	*284±30*	*30.9±3.3*
1 ●	13 November 1960	19	229	Day 2 [63] Large SEP events also seen [3,4,5,6,10] widespread aurora [6,37,48]	249	10.51
2 ●	18 September 1941	17	269	Day 1 of the "Geomagnetic Blitz" [12,13,3,4,48,63] (a.k.a. the "Playoff Storm" [14]) From aa, one of the 3 largest storms in that solar cycle [70]	239	14.17
3 ●	13 March 1989	22	97	Day 1, Hydro Quebec Power Loss Event [8,9,4,3,48,63]. From aa, one of the 3 largest storms in that solar cycle [70]	234	12.02
4 ●	24 March 1940	17	220	Day 1, the "Easter Sunday" Storm, First power grid effect detection [21,23,48,57,63]	220	13.68
Est 1 ▲	*03 September1859*	*9*	*104*	*Peak of "Carrington" event* [1,45,46,48]	*215±23*	*19.5±2.1*
5 ●	25 March 1940	17	220	Day 2, the "Easter Sunday" Storm, First power grid effect detection [21,23,48,57,63]	212	13.19
Est 1. ▲	*23 July 2012*	*24*	*133*	*STEREO-A event* [2]	*211±23*	*23.0±2.5*
6 ●	29 October 2003	23	220	Day 1, "Halloween" Events [16,24] GICs [25,48,63]	206	9.47
7 ●	08 February 1986	21	346	Day 1, flares followed by storm [5,33,3,4, 36, 48,63] From aa, one of the 3 largest storms in that solar cyle [70]	203	16.27
8 ●	12 November 1960	19	229	(Day 1 of 2) Large SEP events also seen [3,4,5,6,10,63] widespread aurora [6]	202	8.54
9 ●	06 October 1960	19	225	[3, 31,48]	202	8.53
10 ●	19 September 1941	17	269	Day 2 of "Geomagnetic Blitz" [11,12,4,48,63] From aa, one of the 3 largest storms in that solar cyle [70]	199	11.81
11 ●	01 April 1960	19	207	SEP events [10,3,39] Major Dst storm [63]	195	8.25
12 ●	07 October 1960	19	226	[3,31]	194	8.21
13 ●	15 July 1959	19	181	Day 1, [48,63] Aurora, telegraph and SW disruption [11,3], SEP events [6,10,63]	187	8.78
14 ●	14 March 1989	22	97	Day 2, Hydro Quebec Power Loss Event [8,9,4,3]	184	9.48
15 ●	31 October 2003	23	220	Day 3,"Halloween" Events [16,24] Large GIC [25,48,63]	181	8.32
16 ●	01 March 1941	17	251	Day 1. Widespread aurora [3,27,30,48,63]	180	10.66
17 ●	26 May 1967	20	87	Day 2 of the "1967 Great Storm" [18,3,48,63] SEPs [9]	177	14.81
18 ●	07 February 1946	18	58	Day 1, storms predicted. Bombay, Lisbon, Cairo, and Singapore report telegraph disturbances. Aurora seen over New York City. Complete blackout of HF radio signals for second day [38,48,60,63]	177	9.51

19	●	30 March 1940	17	221	Day 2, Re-intensification of the “Easter Sunday” Storm, First power grid effect detection [21,23,3,4,48]	177	10.99
20	●	11 February 1958	19	130	Day 2 of 2: Major SW radio effects and aurora [20,3,48, 56,63]	176	9.17
21	●	10 November 2004	23	251	Large GICs [25, 40]	173	12.93
22	●	25 May 1967	20	87	Day 1 of the “1967 Great Storm” [18,3,48,63] SEPs [9]	172	14.39
23	●	14 July 1982	21	217	[33,3,4,48] Major Dst storm [63]	171	7.61
24	●	09 November 2004	23	251	[40]	171	12.72
25	●	30 October 2003	23	220	Day 2, “Halloween” Events [16,24] Large GIC [25,48,63]	170	7.8
26	●	28 March 1946	18	63	Major SW radio effects and aurora [14,3,4,48,60,63] From aa, one of the 3 largest storms in that solar cyle [70]	169	9.1
27	●	04 September 1957	19	114	Day 2, [3,4,42,48] aurora in Chicago [43] Major Dst storm [63]	168	8.35
28	●	05 August 1972	20	243	Day, 2 the “Space Age Storm” Predicted from flare observations, CME detected by Pioneer 9 [4]. Between Apollo 16 and 17 misions [28,3,4, 48,63] From aa, one of the 3 largest storms in that solar cyle [70]	167	13.28
29	●	29 March 1940	17	221	Day 1, Re-intensification of the “Easter Sunday” Storm, First power grid effect detection [21,23,3,4,48]	167	10.37
30	●	09 February 1986	21	346	Day 2, flares followed by storm [5,33,3,4, 36, 48,63] From aa, one of the 3 largest storms in that solar cyle [70]	166	13.32
31	●	05 July 1941	17	262	Major SW radio effects and aurora [14,15,3,48,63]	165	9.78
32	●	22 September 1946	18	80	[3,48,60,63]	165	8.84
33	●	31 March 1960	19	207	[39,48,63]	163	6.87
34	●	08 July 1958	19	145	Day 1, Greatest IGY storm [32,3,48,63]	160	8.35
35	●	27 July 1946	18	74	First published link to GLEs SEPs [14, 3,60]	158	8.49
36	●	13 July 1982	21	217	[41] Major Dst storm [63]	157	6.99
37	●	25 March 1946	18	62	Major HF radio effects and aurora [4,48,60] From aa, one of the 3 largest storms in that solar cyle [70]	154	8.28
38	●	26 July 1946	18	74	[47, 48,60,63]	154	8.28
39	●	08 February 1946	18	58	Day 2, storms predicted. Bombay, Lisbon, Cairo, and Singapore report telegraph disturbances. Aurora seen over New York City. Complete blackout of HF radio signals for second day [38,48,60,63]	153	8.21
40	●	20 August 1950	18	221	Day 2 [48] Widespread aurora [52]	153	8.45
41	●	06 September 1982	21	223	[33,3,4,48]	152	6.79
42	●	08 November 1991	22	193	Day1 [44.63]	150	6.42
43	●	31 March 2001	23	142	[34,63]	149	11.55
44	●	09 July 1958	19	145	Day 2, Greatest IGY storm [32,3,48,63]	149	7.76
45	●	05 September 1957	19	114	Day 3 [3,4,48]	149	7.43
46	●	09 November 1991	22	193	Day 2 [44,63]	148	6.29

47	●	20 November 2003	23	222	Day 1, Large GIC [25]	147	6.73
48	●	27 March 1959	19	170	[3]	146	6.84
49	●	27 July 2004	23	242	[25]	145	10.85
50	●	19 August 1950	18	221	Day 1 [48] Widespread aurora [52]	145	8.01
51	●	16 July 1959	19	181	Day 2 [48,63]	145	6.78
52	●	12 May 1949	18	175	[48,60]	145	9.37
53	●	05 June 1991	22	177	[5,22,3,48]	144	6.16
54	●	10 February 1958	19	130	Day 1 of 2: Major SW radio effects and aurora [20,3,48, 56,63]	144	7.5
55	●	24 March 1991	22	170	Day 1 [5,3,58,59]	144	6.14
56	●	16 July 2000	23	121	Day 2, “Bastille” Storm, Large GICs [25.48] Major Dst storm [63]	143	9.47
57	●	15 July 2000	23	121	Day 1, “Bastille” Storm, Large GICs [25.48] Major Dst storm [63]	143	9.47
58	●	22 September 1957	19	116	Day 1. [3,4]	143	7.11
59	●	10 May 1992	22	211	[35.48]	142	8.62
60	●	08 November 2004	23	251	[40]	142	10.6
61	●	05 February 1983	21	238	[49]	141	7.6
62	●	23 September 1957	19	116	Day 2, [3,4] Major Dst storm [63]	140	6.98
63	●	25 January 1949	18	164	Day 1, Widespread aurora [26,60,63]	140	9.06
64	●	26 January 1949	18	165	Day 2, Widespread aurora [26,60,63]	139	9.02
65	●	07 November 2004	23	251	[40]	139	10.34
66	●	21 November 2003	23	222	Day 2, Large GIC [25]	139	6.36
67	●	27 April 1956	19	66	[50]	138	7.67
68	●	02 March 1941	17	251	Day 2. Widespread aurora [3,27,30,48,63]	137	8.13
69	●	18 July 1959	19	182	Day 4 [48,63]	137	6.41
70	●	08 March 1970	20	170	SEPs seen [9], Dst storm and TEC depletion [61]	135	11.33
71	●	17 July 1959	19	181	Day 3 [48,63]	135	6.32
72	●	25 March 1991	22	170	Day 2 [5,3,58,59] Major Dst storm [63]	135	5.75
73	●	30 June 1957	19	108	[60]	135	6.7
74	●	01 November 1968	20	130	[64]	134	9.89
75	●	25 January 1938	17	149	Day 1 of the “Fatima Storm” [4,29,63] Ap > 100 on 17, 22, and 25 January, widespread aurora on 25 January including in the Azores and north Africa [51]	131	8.6
76	●	21 October 1989	22	119	Low latitude red aurora [62]	131	6.74
77	●	20 October 1989	22	119	Low latitude red aurora [62]	131	6.73
78	●	15 October 1949	18	190	[69]	131	8.47
79	●	03 September 1966	20	65	SEP [10]	131	12.74
80	●	25 September 1951	18	260	[66]	130	5.84
81	●	02 November 1968	20	130	SEP [10]	130	9.63
82	●	16 August 1959	19	184	SEP [10]	130	6.09

83	04 September 1958	19	150	Widespread aurora in Europe [54] Major Dst storm [63]	130	6.74
84	04 September 1966	20	65	SEP [10]	130	12.64
85	30 April 1960	19	210	[4, 39,10] Major Dst storm [63]	129	5.46
86	28 October 1991	22	192	GIC [65]	129	5.51
87	04 August 1972	20	243	Day, 1 the “Space Age Storm” Predicted from flare observations, CME detected by Pioneer 9 [4] Between Apollo 16 and 17 misions [28,3,4,48,63]. From aa, one of the 3 largest storms in that solar cyle [70]	127	10.05
88	23 April 1946	18	65	[60,63]	126	6.77
89	26 January 1938	17	150	Day 2, of the “Fatima Storm” [4,29,63] Ap > 100 on 17, 22, and 25 January, widespread aurora on 25 January	126	8.23
90	04 February 1983	21	237	SEP [10]	125	6.75
91	03 September 1957	19	114	Day 1, [3,4,48] Major Dst storm [63]	125	6.24
92	03 March 1947	18	96	[60]	125	6.64
93	22 September 1963	19	332	SEP [10]	123	9.8
94	13 September 1957	19	115	Auroral event [63,68]	123	6.12
95	16 May 1956	19	67		122	6.77
96	21 February 1994	22	275	[67]	122	6.71
97	25 July 1981	21	182	SEP [10]	122	7.46
98	24 April 1946	18	65	[60]	121	6.5
99	29 September 1957	19	117	[4] Widespread aurora in Europe [53] SEP [10]	121	6.02
100	21 February 1950	18	203	Disruption to cable service [55,60]	121	6.68
≥101	The remaining 30947 daily $[Ap_C*]_{MAX}$ values (97.68% of all available values for 1932-2017, inclusive)					

1. Shea, M.A. and D.F. Smart (2006) Compendium of the eight articles on the “Carrington Event” attributed to or written by Elias Loomis in the American Journal of Science, 1859-1861, Adv. Space Res., 38 (2), 313-385, doi: 10.1016/j.asr.2006.07.005.
2. Baker, D. N., X. Li, A. Pulkkinen, C. M. Ngwira, M. L. Mays, A. B. Galvin, and K. D. C. Simunac (2013), A major solar eruptive event in July 2012: Defining extreme space weather scenarios, Space Weather, 11, 585–591, doi:10.1002/swe.20097
3. Bell, J. T., M. S. Gussenhoven, and E. G. Mullen (1997) Super storms, J. Geophys. Res., 102 (A7), 14189–14198, doi:10.1029/96JA03759.
4. Lefèvre, L., S. Vennerstrøm, M. Dumbović, B. Vršnak, D. Sudar, R. Arlt, F. Clette, N. Crosby (2016) Detailed Analysis of Solar Data Related to Historical Extreme Geomagnetic Storms: 1868 – 2010, Solar Phys, 291, 1483–1531, doi: 10.1007/s11207-016-0892-3
5. Steljes, J.F., H. Carmichael, and K.G. McCracken (1961) Characteristics and fine structure of the large cosmic-ray fluctuations in November 1960, J. Geophys. Res., 66, 1363–1377, doi: 10.1029/jz066i005p01363
6. Smart, D.F and M.A Shea (1996) Solar-interplanetary circumstances associated with the major events in March and June 1991 and comparison with similar events of previous solar cycles, Adv. Space Res., 17 (2), 147-15, doi: 10.1016/0273-1177(95)00526-K
7. Newspaper report: “Blast on Sun Treats U.S. to Aurora Borealis”, New York Herald Tribune (European Edition, Paris, France), Tuesday, November 15, 1960, p.5.
8. Shirochkov, A.V., L.N. Makarova, V.D. Nikolaeva, A.L. Kotikov (2015) The storm of March 1989 revisited: A fresh look at the event, Adv. Space Res., 55 (1), 211 – 219, doi: 10.1016/j.asr.2014.09.010
9. Bolduc, L. (2002) GIC observations and studies in the Hydro-Québec power system, J. Atmos. Sol. Terr. Phys., 64, 1793–1802, doi:10.1016/S1364-6826(02)00128-1.

10.	Shea, M.A. and D. F. Smart (1990) A summary of major solar proton events, Solar Physics, 127 (2), 297 – 320, doi: 10.1007/bf00152170
11.	Newspaper report: "Radio Upset By Magnetic Disturbance", Chicago Daily Tribune Jul 16, 1959
12.	Love, J. J., and P. Coïsson (2016), The geomagnetic blitz of September 1941, Eos, Trans. Am. Geophys. Union, 97, doi: 10.1029/2016EO059319
13.	McNish, A.G. (1941) Auroral display and geomagnetic storm of September 18-19, 1941, Science, 94 (2444), 413 – 414, doi: 10.1126/science.94.2444.413
14.	Newspaper reports collected at Solar Storms.Org "Space Weather Newspaper Archives" http://www.solarstorms.org/SRefStorms.html
15.	Newspaper report: "Aurora Borealis Slows War News", The Washington Post, Jul 6, 1941
16.	Lopez, R.E. D.N. Baker, and J. Allen (2004) Sun unleashes Halloween storm, Eos, Trans. Am. Geophys. Union, 85 (11) 105, doi: 10.1029/2004eo110002
17.	Huttunen, K. E. J., H.E. Koskinen, T.I., Pulkkinen, A. Pulkkinen, M. Palmroth, E.G.D., Reeves, and H. J. Singer, (2002), April 2000 magnetic storm: Solar wind driver and magnetospheric response, J, Geophs Res., Space Physics, 107 (A12), SMP 15, 1-21, doi: 10.1029/2001ja009154
18.	Knipp, D. J., et al. (2016), The May 1967 great storm and radio disruption event: Extreme space weather and extraordinary responses, Space Weather, 14, 614–633, doi:10.1002/2016SW001423.
19.	Forbush, S.E. (1946) Three Unusual Cosmic-Ray Increases Possibly Due to Charged Particles from the Sun, Phys. Rev., 70 (9/10), 771 – 772, doi: 10.1103/physrev.70.771
20.	Lawn V.H. (1958) Aurora Borealis Blacks Out Radio; Global Communications Cut as Brilliant Display Lights Up Skies Over U. S., New York Times, 11 February, p62
21.	Nature's Prank Upsets The Air, New York Times Mar 31, 1940
22.	Kozyra, J. U., M. W. Liemohn, C. R. Clauer, A. J. Ridley, M. F. Thomsen, J. E. Borovsky, J. L. Roeder, V. K. Jordanova, and W. D. Gonzalez (2002) Multistep Dst development and ring current composition changes during the 4–6 June 1991 magnetic storm, J. Geophys. Res., 107 (A8), 1224, doi: 10.1029/2001JA000023.
23.	McNish, A. G. (1940), The magnetic storm of March 24, 1940, Terr. Magn. Atmos. Electr., 45 (3), 359–364, doi:10.1029/TE045i003p00359
24.	Pulkkinen, A., S. Lindahl, A. Viljanen, and R. Pirjola (2005) Geomagnetic storm of 29–31 October 2003: Geomagnetically induced currents and their relation to problems in the Swedish high-voltage power transmission system, Space Weather, 3, S08C03, doi:10.1029/2004SW000123.
25.	Juusola, L., A. Viljanen, M. van de Kamp, E. I. Tanskanen, H. Vanhamäki, N. Partamies, and K. Kauristie (2015) High-latitude ionospheric equivalent currents during strong space storms: Regional perspective, Space Weather, 13, 49–60, doi:10.1002/2014SW001139
26.	Aurora Borealis Seen in West Europe's Skies, New York Herald Tribune (European Edition) (Paris, France), Thursday, January 27, 1949, Issue 20529, p.3.
27.	UK Air Ministry/Met Office Observatories' yearbook for 1941 (HMSO 1958)
28	Lockwood, M., and M.A. Hapgood (2007) The rough guide to the Moon and Mars, Astron. & Geophys., 48, 11-17, doi: 10.1111/j.1468-4004.2007.48611.x
29.	Hess, V.F., R. Steinmaurer, A. Demmelmair (1938) Cosmic Rays and the Aurora of January 25-26, Nature, 141, (3572), 686-687, doi: 10.1038/141686a0
30.	Chapman, S. (1957) The Aurora in Middle and Low Latitudes, Nature, 179 (4549), 7-11, doi: 10.1038/179007a0
31.	Brautigam, D. H., and J. M. Albert (2000) Radial diffusion analysis of outer radiation belt electrons during the October 9, 1990, magnetic storm, *J. Geophys. Res.,* **105** (A1), 291–309, doi:10.1029/1999JA900344.
32.	Davis, T. N., and R. Parthasarathy (1967) The relationship between polar magnetic activity DP and growth of the geomagnetic ring current, *J. Geophys. Res*., **72** (23), 5825–5836, doi:10.1029/JZ072i023p05825.
33.	Tsurutani, B. T., W. D. Gonzalez, F. Tang, and Y.T. Lee (1992) Great magnetic storms, Geophysical Research Letters, 19 (1), 73-76, doi: 10.1029/91GL02783
34.	Skoug, R. M., et al. (2003),Tail-dominated storm main phase: 31 March 2001, J. Geophys. Res., 108, 1259, doi:10.1029/2002JA009705, A6.

35.	Shiokawa, K., K. Yumoto, Y. Tanaka, T. Oguti, and Y. Kiyama (1994) Low-latitude auroras observed at Moshiri and Rikubetsu (L= 1.6) during magnetic storms on February 26, 27, 29, and May 10, 1992, Journal of geomagnetism and geoelectricity, 46 (3) 231-252 doi: 10.5636/jgg.46.231
36.	Garcia, H. A. & M. Dryer (1987) The solar flares of February 1986 and the ensuing intense geomagnetic storm, Solar Physics, 109 (1), 119-137
37.	November 13, 1960 Newspaper reports. New York Times, November 14, 1960 p. 14; New York Times, November 13, 1960, p. 3 ;Chicago Daily Tribune, November 14, 1960, p.1; Chicago Daily Tribune, November 16, 1960, p. 16; The Washington Post, November 13, 1960, p. A1; The Washington Post, November 14, 1960, p. A3.
38.	February 3, 1946 reports: Magnetic storms predicted to 'sweep earth' for next 12 days. Began with radio reception problems. Bombay, Lisbon, Cairo, and Singapore report telegraph disturbances. Som problems lasted into March [New York Times, February 3, 1946]. Green curtains, sheets and rays seen over New York City. Complete blackout of HF radio signals on second day. [New York Times, February 8, 1946, p. 18]
39.	Chinburg, D. L. (1960), Great magnetic storm of March 31–April 3, 1960, *J. Geophys. Res.*, 65(7), 2206–2208, doi: 10.1029/JZ065i007p02206.
40.	Trichtchenko, L., A. Zhukov, R. van der Linden, S. M. Stankov, N. Jakowski, I. Stanisławska, G. Juchnikowski, P. Wilkinson, G. Patterson, and A. W. P. Thomson (2007), November 2004 space weather events: Real-time observations and forecasts, *Space Weather*, 5, S06001, doi: 10.1029/2006SW000281.
41.	Parsignault, D. R., J. Feynman, J., & P. Rothwell (1983) The large magnetic storm of July 1982 - A preliminary study, *in International Cosmic Ray Conference*, 18th, Bangalore, India, August 22-September 3, 1983, Late Papers. Volume 10 (A85-22801 09-93). Bombay, Tata Institute of Fundamental Research, 1983, p. 266-269. http://adsbit.harvard.edu/full/1983ICRC...10..266P
42.	Finch, H. F. & P.S. Laurie (1958) Solar activity and geomagnetic storms, 1957, The Observatory, 78, 40-42 http://adsabs.harvard.edu/full/1958Obs....78...40F
43.	Newspaper report: [Chicago Daily Tribune, September 5, 1957, p. 1]
44.	Cliver, E. W., K. S. Balasubramaniam, N. V. Nitta, and X. Li (2009), Great geomagnetic storm of 9 November 1991: Association with a disappearing solar filament, J. Geophys. Res., 114, A00A20, doi:10.1029/2008JA013232.
45.	Green, J.L. and S. Boardsen (2006) Duration and extent of the great auroral storm of 1859. *Advances in Space Research*, *38*(2), 130-135.
46.	Tsurutani, B. T., W. D. Gonzalez, G. S. Lakhina, and S. Alex (2003), The extreme magnetic storm of 1–2 September 1859, *J. Geophys. Res.*, 108, 1268, doi: 10.1029/2002JA009504, A7.
47.	Newspaper reports: Aurora seen over New York, Philadelphia and identified with sunspots now on sun. [New York Times, July 27, 1946, p. 23], Chicagoans see sky alight with auroral display [Chicago Daily Tribune, July 27, 1946. p. 5].
48.	Kappenman, J. G. (2005), An overview of the impulsive geomagnetic field disturbances and power grid impacts associated with the violent Sun-Earth connection events of 29–31 October 2003 and a comparative evaluation with other contemporary storms, Space Weather, 3, S08C01, doi: 10.1029/2004SW000128.
49.	Used in study of effect of storms on thermosphere and mesospheric winds: Singer, W., J. Bremer, P. Hoffmann, A.H. Manson, C.E. Meek, R. Schminder, D. Kürschner, Y.-I. Portnyagin, N.A. Makarov, H.G. Muller, and E.S. Kazimirovsky, E.S. (1994) Geomagnetic influences upon tides—winds from MLT radars. *J. Atmos. and Terr. Phys.*, 56(10), 1301-1311.
50.	Newspaper report: Northern lights stage rare unseasonal show [New York Times, April 27, 1956, p. 8].
51.	Vallance Jones, A., Historical review of great aurora (1992) *Can. J. Phys*., 70, 479-487.
52.	Newspaper report: The Manchester Guardian (1901-1959); Manchester (UK) 21 Aug 1950: 7.
53.	Newspaper report: The Manchester Guardian (1901-1959); Manchester (UK) 30 Sep 1957: 1.
54.	Newspaper report: The Times (London, England), Friday, Sep 05, 1958; pg. 10; Issue 54248.
55.	Newspaper report: New York Times, (New York, USA) February 21, 1950 p. 5
56.	Akasofu, S.-I. and S. Chapman (1962) Large-scale auroral motions and polar magnetic disturbances—III: The aurora and magnetic storm of 11 February 1958. J. Atmos. and Terr. Physics, 24 (9), 785-796.
57.	Nicholson, S. B. (1940) The Great Magnetic Storm of March 24, 1940, Publications of the Astronomical Society of the Pacific, 52, 307, 169. http://adsabs.harvard.edu/full/1940PASP...52..169N

58.	Le, G. M., Z.H. Ye, J.H. Gong, Y.H. Tan, H. Lu, & Y.Q. Tang (2003) Time Determination of March 1991's CME Hitting Magnetosphere, Proc. 28th Int. Cosmic Ray Conf. July 31-August 7, 2003, Trukuba, Japan. Eds: T. Kajita, Y. Asaoka, A. Kawachi, Y. Matsubara and M. Sasaki, p.3601. http://adsabs.harvard.edu/full/2003ICRC....6.3601L
59.	Smart, D.F., M.A. Shea, E.O. Flückiger, and B. Sanahuja (1995) Solar, interplanetary, and geomagnetic phenomena in March 1991 and their association with spacecraft and terrestrial problems. *Nuclear Physics B-Proceedings Supplements*, *39* (1), pp.26-34.
60.	Matsushita, S. (1959). A study of the morphology of ionospheric storms. *Journal of Geophysical Research*, **64** (3), 305-321
61.	Lanzerotti, L. J., L. L. Cogger, and M. Mendillo (1975), Latitude dependence of ionosphere total electron content: Observations during sudden commencement storms, *J. Geophys. Res.*, **80** (10), 1287–1306, doi: 10.1029/JA080i010p01287
62.	Oguti, T. (1992) A review of the October 21, 1989 red aurora seen in Japan and from the AKEBONO (EXOS-D) satellite, Canadian Journal of Physics, 70 (7), 488-499, doi: 10.1139/p92-084
63.	Cliver, E.W. and L. Svalgaard (2004) The 1859 solar–terrestrial disturbance and the current limits of extreme space weather activity, *Solar Physics*, **224** (1-2), 407-422.
64.	Russell, C. T., C. R. Chappell, M. D. Montgomery, M. Neugebauer, and F. L. Scarf (1971), Ogo 5 observations of the polar cusp on November 1, 1968, *J. Geophys. Res*., **76** (28), 6743–6764, doi: 10.1029/JA076i028p06743.
65.	Bolduc, L. (2002) GIC observations and studies in the Hydro-Québec power system, J. Atmos.Sol.-Terr. Physics, 64 (16), 1793-1802
66.	Newspaper report: [Los Angeles Times, September 23, 1951, p. 48].
67.	J. T. Gosling, D. J. McComas, J. L. Phillips, V. J. Pizzo, B. E. Goldstein, R. J. Forsyth, R. P. Lepping (1995) A CME-driven solar wind disturbance observed at both low and high heliographic latitudes, Geophys. Res. Lett., 22 (13), 1753-1756, doi: 10.1029/95gl01776
68.	Newspaper report: [Los Angeles Times, September 13, 1957, p. 1].
69.	Newton, H. W. (1949) Council report on solar activity in 1949 : Sunspots, *Monthly Notices of the Royal Astronomical Society,* 110, p.169-170, http://adsbit.harvard.edu//full/1950MNRAS.110..169N/0000170.000.html
70.	Willis, D.M. P. R. Stevens, S. R. Crothers (1979) Statistics of the largest geomagnetic storms per solar cycle (1844-1993), *Ann. Geophys*., 15 (6), 719-728, DOI: 10.1007/s00585-997-0719-5